JOURNAL OF MATERIALS SCIENCE **36** (2001) 3143–3164

Review
Spherulites: A personal perspective*

J. H. MAGILL
Materials Science and Engineering Department, School of Engineering, University of Pittsburgh, Pittsburgh, PA, 15216, USA
E-mail: magill@engrng.pitt.edu

Chain-folding is a central feature of the self-organizational aspect of polymer in the solid state, yet the ability of a polymer chain to organize into a folded morphology depends upon its length. The shorter chains seem to fold with relative ease in dilute solution crystallization, but in the melt where topological constraints are encountered, spherulitic crystallization is less facile especially in the higher molecular weight fractions. Polymer morphology and properties demonstrate this point clearly according to the experimental evidence, obtained from several sources and presented in this article. For topological and statistical reasons, longer chains are responsible for more interfacial disorder if the degree of crystallinity, density, mechanical behavior, "fold" surface free energy, "transition" from brittleness to toughness, and so on, may be used as guidelines. Spherulites of homopolymers or copolymers are undoubtedly less ordered than crystals of comparable MW fractions, if measured properties are a manifestation of morphology. The imperfections in spherulites are mainly associated with the quasi-amorphous interlamellar regions within them. Polymer crystallinity decreases as the molecular weight of polymer fractions increase at comparable crystallization temperatures or undercooling conditions. This trend is true for all polymers that have been studied extensively.

Prologue

I spent two six-week periods as a graduate summer employee about the mid 1950s at the ICI Dyestuffs Division, Blackley, Manchester, UK, but I never met Andrew Keller there. A few years afterwards when in the employment of British Nylon Spinners (BNS) in Pontypool, South Wales I had prepared some very thin crystalline platelets of several polyamides by means of melt crystallization in a wedge-like geometry at relatively small undercooling. Under the optical microscope they were uniformly self-extinguishing in the optical microscope and superficially reminiscent of polycrystalline metallic grains. Peter Harris and I suspected that they might be "single crystals" but we needed an electron microscope. In due course, arrangements were made with Prof. M. H. L. Pryce, F.R.S, Chairman of the H.H. Wills Physics Laboratory, to use their electron microscope at Bristol. This may have been the same instrument that Andrew Keller had used to investigate his first solution-grown polyethylene single crystals. Anyhow, Harris and I were pleased to discover that our thin polyamide films displayed several orders of diffraction! Shortly afterwards, while still in the employment of BNS, an ICI subsidiary, I attended an evening lecture presented by Andrew Keller at the Royal Society of Chemistry, London, UK in the early 1960s. Here I met him for the first time. His topic was "The Morphology of Polymers," formation, sectorization, truncation and heat treatment of crystals of polyethylene and spherulites of other polymers. I was intrigued! I had better be, since I had to write a report upon my return to BNS before being reimbursed for my expenses! No reason, just company policy! Afterwards, we often met at meetings and conferences, and this association led to my spending a sabbatical leave during 1975–76 at the H. H. Wills Physics Laboratory. The discussions over the morning coffee and afternoon tea, an entrenched custom at the Bristol laboratory, proved to be exciting at times. With Professors Andrew Keller and Sir Charles Frank often present, what else could they be but interesting, not to mention input from other lively faculty and keen researchers?

Andrew and his wife Eva were good friends of ours and remained so until their early demise.

1. Introduction

Spherulites as polycrystalline moieties in materials, predate historical records. Now, it is known that they are found in volcanic rocks [1], silicate minerals [2], metals [3], rhyolites [4], elemental materials [5], simple organic molecules [6], natural [7] which are indigenous

* In memory of Andrew Keller.

Figure 1 Floreal-looking nylon 4, 9 negatively birefringent spherulites crystallized from the melt at 235°C (16 hr). Fusion temperature 267°C (1/2 hr); ×128.

throughout our world and even on other planets*, and unnatural (i.e. synthetic) macromolecules of diverse kinds [8]. Nowhere are they more prevalent than in the new materials of the 20th century, i.e. diverse kinds of synthetic polymers, namely homopolymers [9], copolymers [10], polymer blends [11], and mesophase polymers [12]. Are these similar in kind but different in detail, is a questions that needs to be resolved?

Perhaps the oldest study of spherulites leads back to the 19th century when Lehmann [13] described them as being comprised of fibrillar crystal arrays radiating from a common central nucleus, thus creating a spherical aggregate. Now, we realize that they are almost ubiquitous in semi-crystalline synthetic macromolecules, whether they are crystallized from the supercooled melt or from moderately supersaturated polymeric solutions or gels and so on. Even though they are universally recognizable in the optical microscope, a unique description of their formation and growth is not yet complete, despite the fact that they are technologically important and in many ways responsible for the solid state properties of many plastic materials. Since their presence is not always beneficial, attempts are often made to reduce or control them in diverse ways in regard to their size and distribution [14]. Sometimes they are almost eliminated from commercial products whenever they interfere with mechanical properties and transparency, for example. Their optical textures are also various and are sometimes floreal or aesthetic-looking, but their morphologies at times, appear to be complex and not well understood (see Fig. 1).

The morphogenesis of spherulites grown in viscous media (i.e. gels) was first tackled by two mineralogists, Morse and Donnay [15] whose optical studies sparked an interest in this area. They demonstrated that spherulitic growth occurs whenever dissolved inorganic salts are "crystallized" from a viscous gel. Somehow, this procedure compromises regular facetted crystal growth and instead produces spherulites that are polycrystalline. We shall return to this point for an account of the behavior of small inorganic molecules in supercooled melts. Later on, spherulites were found to be abundant in semi-crystalline polymers and in natural materials such as biopolymers. With the advent of World War II, national needs sparked industrial investments in synthetic polymers as substitutes for natural

* Located in moon rocks.

materials such as rubber, silk, etc. most of which had to be imported. The discovery at that time that man-made products were often superior in their mechanical performance to natural ones, led to a new polymer industry, that changed our lives and living standards in so many ways in the 20th century. Consequently, investigations of polymer morphology, properties and their uses continued to grow to its most recent status as a branch of Materials Science and Engineering Technology.

For instance at ICI, key optical and X-ray structure investigations were carried out by Bunn and his associates [16] in the 1940s employing polyethylene ("Polythene") and polyamides (nylon 6,6 and 6,10) [17]. Herbst [18] introduced micro-beam X-ray diffraction to probe preferred orientation within spherulites. The morphological and other studies by Keller [19–22] and Point [23] revitalized the interest in the texture of spherulites. At this time there were difficulties in explaining some aspects of polymeric behavior based upon the Fringed-Micelle Model (FM) [24] where three dimensional, 3D, crystallites were presumed to be formed by lateral accretion of chains leaving variously disordered regions interspersed between these conjoined 3D moieties. The morphology of these regions (often glassy) is still an open question, since, according to a recent Nobel Laureate, the glassy state still remains a challenge [25].

With the discovery in 1957 by Keller, Till and Fischer of chain-folding in polyethylene crystallization from dilute xylene solution, there was a movement away from the complex FM model. However, the chain-folded model is not without its own difficulties; some of these are mentioned in this article. It is rightful to recognize (as Keller himself indicated [26]) that chain-folding had been invoked in 1938 by Storks [27] in the course of his investigations of thin films of rubber, but interest was found lacking in this work. However Keller's keen pursuit after 1957 of the kinetic aspects of crystal growth with O'Conner [28] and with others [29] established a milestone in macromolecular science. Their work demonstrated that chain-folding and crystal growth are kinetically controlled. Folding was a rate enabling process that permitted crystallization to proceed in a less cumbersome manner than the F-M model had allowed, and also at a moderate rate in many polymers, except at low and large undercoolings. Theories were soon formulated to describe the kinetics of growth rate measurements, but there were difficulties as a recent review indicated [30].

Shortly afterwards, Eppe *et al*. [31], Geil [32], and many others [33, 34] established by electron microscopy and diffraction, that in melt crystallized thin films, the chain molecules were also oriented normal to surface. The analogy between very thin lamellar-like textures ("single crystals") grown from dilute solution and the slightly thicker lamellae found in hedrites, crystalline aggregates and spherulitic films in the bulk crystallization of many different polymers soon followed. In this manner "bridges were built" and morphology flourished! In an attempt to be terse here, we shall return to the spherulites *per se*, but this link is a crucial one in the morphogenesis of solid polymeric structures, although some issues such as crystallinity as a signpost of morphology were not always settled in the minds of some investigators. Other challenges have followed. From this point on, Andrew Keller's research flourished. It was always at the leading edge, but my discourse will be severely restricted here to the morphology of polymer spherulites and its ramifications, not on his many successes in other fields. Still, there will be times when the writer must revert to lamellar crystals in order to maintain the "link" between melt and solution crystallization where many papers have been published. At this point, he apologizes for the numerous omissions that have been made of many other relevant papers in this vast field.

2. Spherulites

Andrew Keller's contributions to our understanding of spherulites started in the early 1950s at ICI, Manchester, England. He never lost sight of the challenges in this field; his last publication on spherulites in the 1990s focused on polyamide 66 negative spherulites, tackling once more a long-standing problem [35, 36] and one which had eluded many, including the writer. His early endeavors focussed on semicrystalline polyamides, polyethers and polyethylenes where he used microscopy (optical and electron), X-ray diffraction (small-angle and wide-angle) to study spherulites and their intricate morphologies.

Briefly, spherulites may be categorized optically using polarized light, into several types that exhibit characteristic properties. Negatively birefringent entities are the most common in synthetic polymers with fibrillar or banded (ringed) extinction patterns, either in distinct spherulites, or for situations where both morphologies may co-exist for instance in polyamides as "mixed spherulites", :see Fig. 2 [37]. If the twisting of radiating lamellae is not co-ordinated only a fibrillar-like texture with well-defined Maltese cross pattern, attests to the symmetry of these polycrystalline moieties, and corresponding to the principal vibration directions of the polarized light with respect to each other. Periodic "in phase" twisting or banding was demonstrated for 50 μm banding in polyethylene by Fujawara [38] by means of optical microscopy and microbeam X-ray diffraction measured from within these spherulites. A case in point is presented for the left-handed spirals highlighted in the ion-etched polyethylene spherulites Fig. 3.

Positively birefringent spherulites are less common than the negatively birefringent class. They too may be ringed or fibrillar (lamellar) with their optical polarizability along the radius being in excess of the mean encountered in the other two principal perpendicular directions of the indicatrices. Polymers with strong dipoles (i.e. H-bonds) have these usually inclined at a large angle to the skeletal chain backbone as in polyamides, and belong to this category [16]. Whenever the lamellar chain axis is tilted and is twisting about an optic axis with respect to the spherulite radius, complex "zig-zag" extinction was illustrated schematically by Keller [39] before uniaxial and biaxial extinction patterns were modeled by Mann and Roldan [40] and

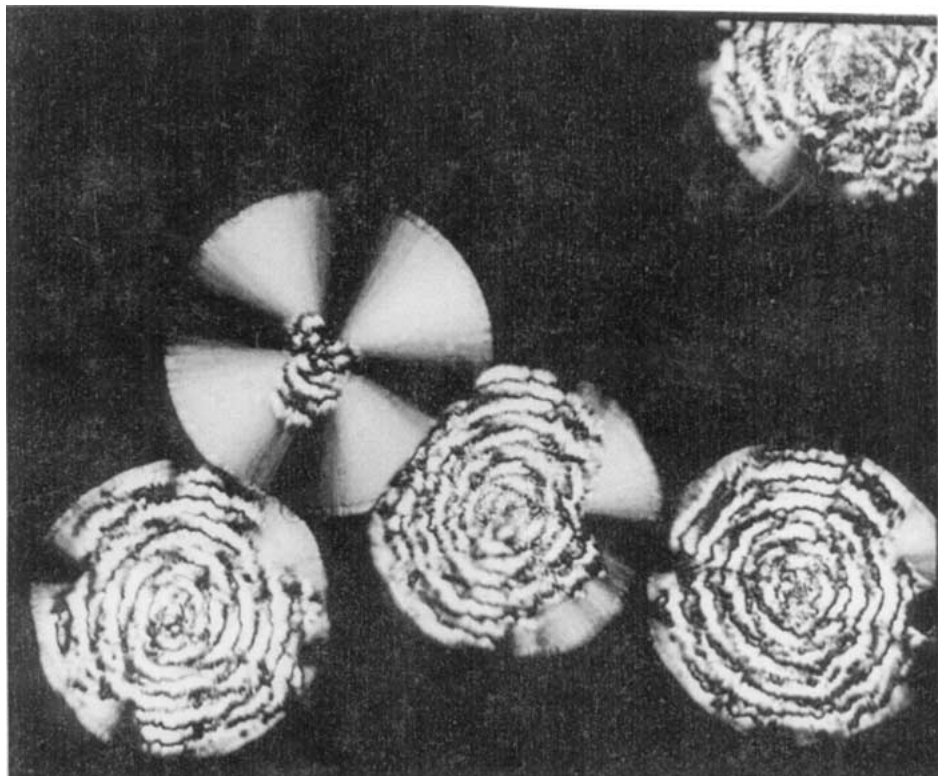

Figure 2 "Mixed" nylon 96 positively birefringent spherulites formed from the melt at 210°C (1/4 hr) after fusion at 270°C (1/4 hr) (Magill, unpublished).

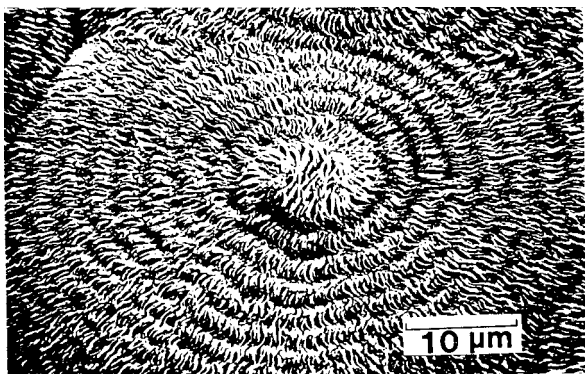

Figure 3 Ion-etched spherulite of melt crystallized HDPE polyethylene with anti-clockwise spiralling. (after Shankernarynan et al. 1987).

Keith and Padden [41], following the theory advanced by Nye [42]. Now thanks to the careful work of Atkins and co-workers, structural aspects of polyamides have been advanced considerably [43].

Another less common category of spherulite is the non-birefringent variety that only arise in a narrow temperature interval where there appears to be a "switch-over" in morphology (see: Diversity—Section 12). Optically, this situation may happen whenever (a) the crystallites within the spherulite are oriented at random or (b) when optical viewing takes place along an optic axis on a Federov stage. In all other orientations it will appear birefringent.

In the interest of brevity, we will not elaborate on other less common, but nonetheless important varieties such as (i) crystalline aggregates (ii) hedrites (iii) chain-extended spherulites (iv) complex spherulites and (v) floreal and other varieties [8] that are referenced elsewhere, some of these will receive attention at appropriate places in this article. The over-riding fact is that spherulites are semicrystalline "composite" materials comprised of at least two phases intimately interspersed with each other in ways that are responsible for properties.

3. Spherulite crystallization

Spherulites frequently nucleate heterogeneously and develop in three dimensions, before impinging upon each other forming polyhedra. Since the depth of focus in the optical microscope is limited, the scanning electron microscope reveals the three dimensional nature of these bodies (see for example Fig. 3). Decades ago Kirchoff [44] reported that Gutta-pencha crystallized at 15°C from a 16% solution in benzene to form "spherulitic dendritic crystals." Several other forms are known to exist in this material. Some are shown in Fig. 4a and b. Unrestricted spherulitic profiles are often obtained by SEM and examples are depicted in Fig. 5a and b for natural rubber [9] and poly (bis-trifluoroethoxy phosphazene) (PBFP) respectively [45]. The growth of spherulites are most conveniently investigated in two-dimensional (2D) geometry between microscope cover-slips. From this vantage point Flory and McIntrye [46] established that 2D spherulites grow by a secondary nucleation mechanism, that may be simply described by

$$G(T) \sim \mathrm{e}^{-\mathrm{K/T\Delta T}} \tag{1}$$

where $\Delta T = T_{\mathrm{m}}^{\circ} - T_{\mathrm{c}}$. $G(T)$ is the interfacial growth rate and K is a geometric parameter depending upon the conditions. This equation does not apply well at the larger undercooling and the influence of MW on

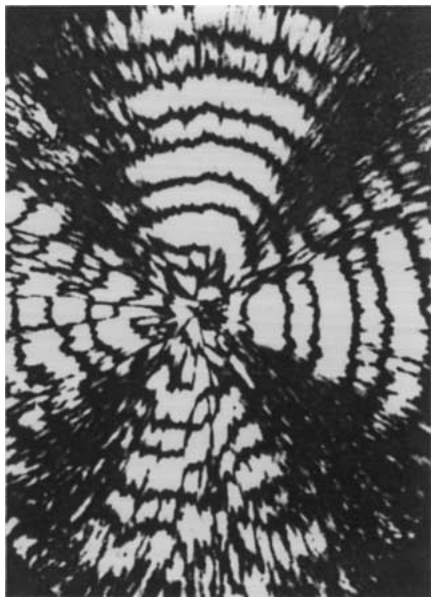

(a)

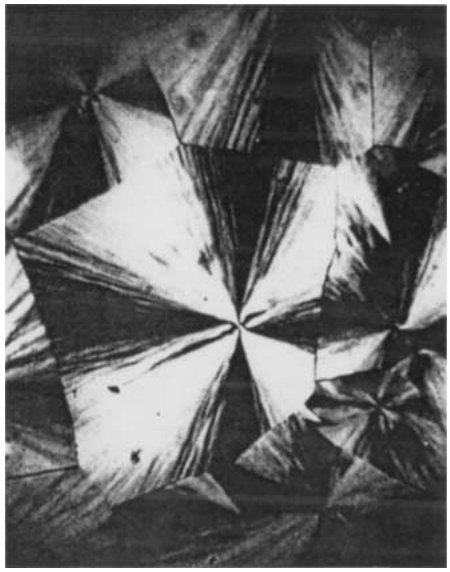

(b)

Figure 4 a) Gutta-percha crystallized from paraffin oil at 42°C. (×285); b) Spherulites of Gutta-percha grown from the melt at 18°C (×270); (after Schuur, 1953.).

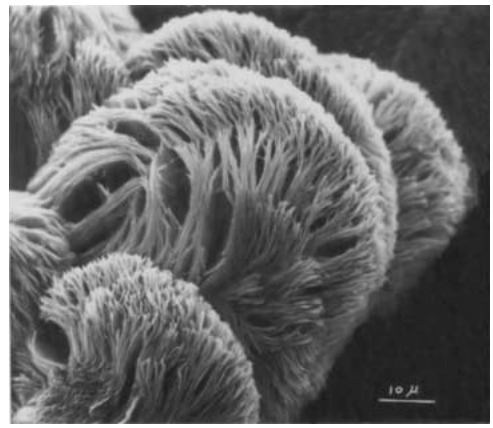

(a)

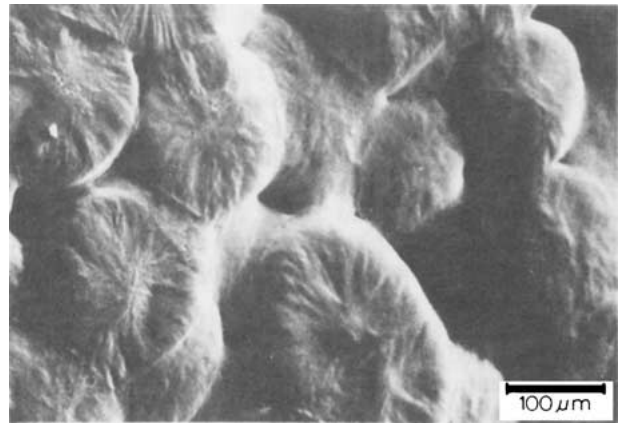

(b)

Figure 5 SEM micrographs of melt crystallized spherulites formed under unrestricted growth conditions: a) trans −1, 4-polyisoprene fraction of Mv = 1.4×10^5 (crystallized from amlyacetate (1% solution) at 20°C and reacted with OsO_4; (Courtesy of A. E. Woodward). b) SEM micrograph of PBFP cast from solution of THF at room temperature; gold sputtered under Ar at 10^{-2} Torr; after Kojima and Magill, Ref. 45).

morphology also needs to be factored into the equation. Mandelkern *et al*. [47] developed a theory for the crystallization rate of macromolecules from the melt and concluded that not only the nucleation rate, but also the spherulitic rate of growth must pass through a maximum with undercooling. Homogeneous nucleation (now known to be incorrect) was presumed. Price [48] pointed out that polymer crystallization (spherulitic) from the melt was a heterogeneous process. Most of this came about before chain–folding was introduced.

In the 1960s Sharples [49] demonstrated that the formation of spherulitic nuclei in polymers (primary nucleation) were pseudo-homonogeneous even in the early stages of growth, because the number of nuclei generated with time, under isothermal conditions, reached a limiting number which was dependent upon the conditions of growth. Others substantiated this result and then went on to exploit heterogeneous control as a procedure for controlling bulk crystallization rate and polymer properties in various ways [14]. The literature in this area is enormous, containing also many patents. However, in recent times the need for nucleation control was questioned by Sadler [50, 51] who proposed that kinetically controlled growth with an activation barrier (a "roughness" model) can be sufficient to mimic the growth rate up to moderate undercooling. Other kinetic theories are mentioned next.

4. Kinetic rate models for spherulites

Most growth rates may be monitored by employing many different techniques that record the change in some property commensurate with the phase transformation taking place under isothermal or non-isthermal crystallization conditions with time, as for example [52]. The earliest quantitative record which demonstrated that the overall isothermal growth rate, in polymers, passes through a maximum with undercooling, was due to Wood and Bekkadahl [53] for spherulites in natural rubber.

Chain folding information of the late 1950s prompted many kinetic theories of polymer crystallization to be written. Simply written, these are an extension of Equation 1 with a translational diffusion term $D(T)$ added, expressed as

$$G(T) \sim f(T)D(T) \qquad (2)$$

The term $f(T)$ is a geometric surface free energy formulation that embodies nucleation/growth of chain folded lamellae that are bounded respectively by σ, the lateral surface free energy (assumed constant) and σ_e, the chain-folded free energy of the surface that pertains to the morphology of ideally folded lamellae in the Hoffman–Lauritzen formulation [30] and in a recent paper more complex forms after several modifications were introduced [54]. In any case, if σ_e is a dominant morphological parameter (not a constant), then its magnitude must change in accordance with the surface or interlamellar morphology of the appropriate system undergoing crystallization. It should depend upon MW which is of critical importance in spherulitic melt crystallization especially. Flux-based kinetic models just mentioned, presume that σ_e is a constant, a practice that has been contrary to experiment for decades [55, 56]. Whatever the geometric model used, it must be a crucial indicator of the surface texture (folded or modified). The overall interfacial surface energy product, $\sigma\sigma_e$, will always increase irrespective of the geometry selected. Polymer properties are molecular weight dependent because growth rate decreases as chain length increases. Properties, which depend upon morphology, are well illustrated for the following fractionated polymers such as poly (*TMPS*) [56, 57], poly(ethylene) [58], poly (ethylene oxide) [59], trans −1, 4-poly(isoprene) [60] that cover MWs from below 10^4 to above 10^6 Daltons approximately. At the lower molecular weights, i.e. below M_c (corresponding to the molar mass between chain entanglements in zero shear melt viscosity, occur around ~25K Daltons for poly (TMPS) [61]). Below M_c intermolecular interactions (responsible for entanglements)

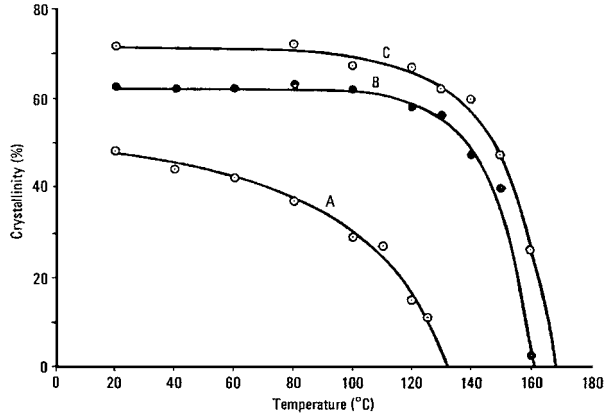

*Figure 6*B Effect of temperature on the crystallinity forms of polypropylene a) is the γ form; b) is the α form and c) is the a highly isotactic form (after Turner-Jones *et al*. Ref. 102).

have little influence on morphology and crystallinity as in Fig. 6A, which represents this situation. The lamellar interfacial free energy, σ_e, however deduced, either from crystallization kinetic models or from SAXS results [62], by employing:

$$\sigma_e = \Delta h_f / 2T_m^\circ \left(\partial T_m / \partial \ell^{-1}\right) \tag{3}$$

where Δh_f is the heat of fusion and ℓ is the crystal thickness is also invariant where few topological constraints are involved; consequently LMW fractions are also brittle. However induced morphology forces σ_e to climb through this M_c region (not a point) where a significant decline in crystallinity begins and continues to higher MW as spherulites become more disorderly. The magnitude of the σ_e term varies almost inversely with the fall-off in crystallinity. Correspondingly, polymer

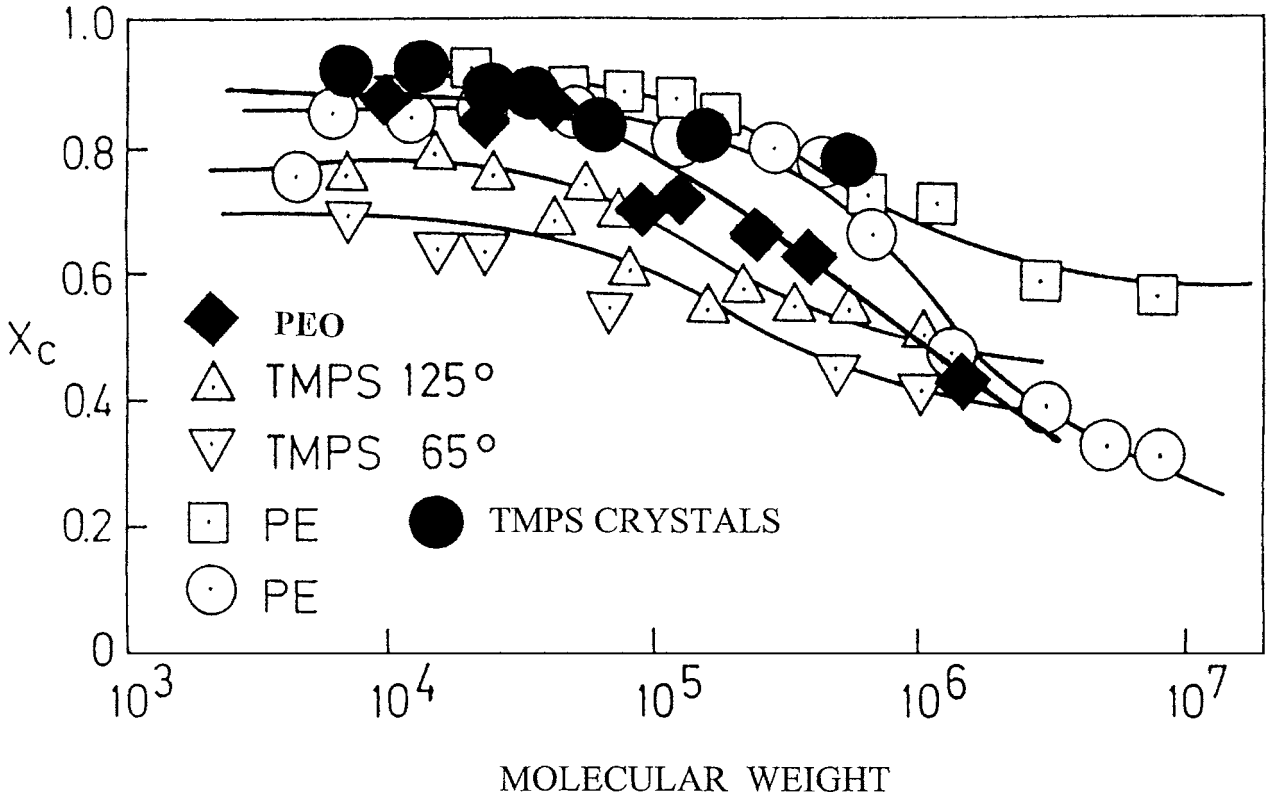

*Figure 6*A Effect of molecular weight on the measured crystallinity of a) poly (TMPS); b) poly(ethylene) c); poly(ethylene oxide) fractions. The weaker dependence of Poly (TMPS) solution grown crystals on MW is included for comparison.

fractions change from being brittle to tough providing a self-consistent correlation. In poly (TMPS) and poly (ethylene oxide) growth rates reflect the changing morphology. Polyethylene is limited as a model system because of its rapid nucleation and growth which only permits limited isothermal measurements to be made over $\sim 25^{\circ}$ of undercooling [30]. Fortunately, its properties have been more extensively investigated, and it is upon these that we have to depend to make our evaluations. The results in Fig. 6A do not rule out chain-folding above M_c, but they certainly demonstrate that morphology and hence properties decline progressively as MW increases. These are experimental facts [55, 56]. The writer finds it difficult to equate a neat fold surface with measured crystallinity (X_c) values as low as 40% or less. Surfaces are more ordered in crystals grown from dilute solution than they are in spherulitic crystallization, even at the higher MWs. This is supported by the connection between surface swelling, surface etching and NMR and other spectroscopic measurements as a function of MW. In this connection Barham *et al*. [63] made an important connection between melt and solution grown crystals relating supercooling and fold length by $l \sim \Delta T^{-1}$. While it is very significant, it does not tell us about influence of MW which is really the issue here, which is a long standing one. The crystallinity of solution and melt crystallized poly (TMPS) depend upon MW as Fig. 6A and [57, 62] show. It seems to the writer that even in a good solvent long polymer chains have some degree of intra-molecular chaos vicinal to the crystal interface, where they must concentrate during nucleation and growth. Intra-molecular and intermolecular entanglements can not be ruled out, otherwise how can surface perturbations and a decrease in crystallinity be accounted for at higher MWs? After all, if a long polymer chain(s) is participating on two separate parts of a substrate—a highly probable event—it will compromise growth and crystallinity. DiMarzio and Gutman acknowledge this situation [64] and our property measurements and analysis support it.

5. Surface swelling

In the writer's opinion an important observation was made by Udagawa and Keller [65] who demonstrated that there is a liquid induced reversible change in the measured long-spacing in polyethylene crystal (lamellar) surfaces and that it was MW dependent. Molecular weights between 2300 and 1.4×10^6 Daltons were investigated. The authors reported a perturbed amorphous fold surface for high MW samples, but somehow overlooked the real implications of this discovery, pointing out a subtle difference in the amount of imbibed solvent for the shorter molecular chain fractions (LMW) as opposed to HMW fractions. SAXS measurements made on swollen as well as dry crystals illustrated that the long period difference ranged from 0.8 nm for the low to 3.5 nm approximately from the highest MW (HMW). In the dry state all the surface features (loops, folds and defects) are collapsed, but in the imbibed condition they are fully swollen (restored to their natural uncollapsed state) with a good solvent. It is easy to estimate that these states may be associated with a crystallinity decrease ranging from about 90 to 77% for HMW and uncollapsed surfaces. The actual values are unimportant, but it is the trend that is significant. Proton NMR (broadline) and other techniques have demonstrated that trend for other polyethylenes, including fractions, studied in this connection [66–68]. Although Udagawa and Keller attached only qualitative significance to their results, the writer finds that this work parallels somewhat related and detailed investigations made in his laboratory for poly (TMPS) fractions over much the same MW range. Poly (TMPS) appears to make a neater fold [69] than is reported for polyethylenes of comparable MWs, but the mean size is still nonetheless elusive. Poly (TMPS) samples were investigated employing selective etching and quantitative spectroscopic investigations with ESCA, FTIR and other standard morphological probes, are to be addressed next.

6. Selective etching

Surface chemical degradation of polyethylene was initiated as a structural probe by Palmer and Cobbald [70] and followed by Peterlin and Meinel [71] Keller and coworkers [72], Williams *et al*. [73] and many others investigating polyethylene. Polypropylene [74] and cellulose [75] were also investigated along similar lines in order to evaluate surface and interface morphology. Polymer bulk (spherulitic) as well as crystal surfaces figured in these studies. Selective surface etching (that severed only exposed –Si-O- bonds on the surface, with no side reactions) was exploited by the writer and associates in order to evaluate the efficacy and selectivity of HF solution [76] and dry diluted HF gas under continuous dynamic flow [77] to selectively removed amorphous surfaces from lamellar crystals and spherulites of poly (TMPS) fractions as a function of chain length. Chain scission kinetics and analysis of surface and bulk morphologies were measured. Spectroscopic, especially ESCA and FTIR techniques provided direct confirmation of the surface chemistry and the kinetics of the surface degradation. X-ray scattering (wide and small-angle) GPC and DSC measurements were also made. For example in a 34,000 Dalton poly (TMPS) [77] single crystal fraction the crystallinity increased from $\sim 75\%$ for the original crystals to $\sim 95\%$ level for the residual crystalline core, after the surface was removed. The fact that there were about 3% of buried folds indicated by a small shoulder on the GPC trace (with chains was about 1.5 times the residual core length of 6.2 nm) may account for the discrepancy from 100%. This number was verified independently by the meticulous GPC work of Dr J. Stejny of the H.H. Wills Laboratory. From these measurements there is little doubt that the lamellar surface is non-crystalline even for this moderately low MW fraction. There may be a mean size attributable to the amorphous surface and it depends upon MW and methods of specimen preparation. For spherulitic interfaces or single crystal surfaces and as well as upon the crystallization conditions which are employed. It is the amorphous surface that exhibits a larger MW dependence than the crystal thickness for the same undercooling, but for increasing MW [62].

Since more disorder is located in the interlamellar regions of spherulites than on surfaces of crystals of the same MW, so that a correspondingly longer HF gaseous etching time is required to remove the interlamellar amorphous material in spherulites as [77] demonstrates, Complementary evidence is also mentioned in Section 4.

7. Decoration of spherulites and interfaces

Gold decoration of crystal and spherulitic surfaces was another useful morphological probe used effectively by Keller and coworkers [73]. The influence of solvent mobilization by a good swelling agent like xylene was also studied (Bassett *et al*. [73]). Fig. 7a and b was used to highlight the surface mobility that may be ascribed to quasi-amorphous surface state. Again, the liquid probe technique relaxes the surface/interfaces to a lesser degree for low as compared with HMW specimens, demonstrating consistency of behavior; see also complementary NMR evidence from Kloos *et al*. [78] and proton NMR related investigations of Berghmann *et al*. [67] and others [68] in verification of the changes in crystallinity with molar mass fractions especially in polyethylenes.

Gold decoration work of poly (TMPS) crystals and fractured spherulitic fractions demonstrated [79] that the fracture surface was more distinct in LMW than it was in HMW homo-polymers fractions. Small-angle X-ray measurements and metal shadowing of crystal mats for TEM height measurements indicated a measurable change in the thickness/lamellar/long period, increasing with MW. Gold decoration techniques used for poly (TMPS) homo and block copolymers [80] pointed up surfaces/interface differences that were confirmed quantitatively by using surface etching with HF (gas or solution), and aided by spectroscopic and X-ray and other analysis.

8. Spherulite-copolymer behavior

Spherulites frequently form from block copolymers, for instance, in random block TMPS/DMS copolymers [81] of comparable MWs ($\sim 10^5$ Daltons). The copolymersed had variable non-crystallizable DMS (dimethyl silicone) block-like content ranging from 0% to 75% as illustrated below:

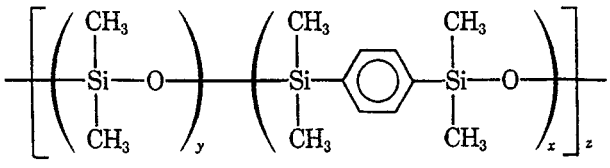

TMPS/DMS copolymer

y = DMS non-crystallizable block $\sim$18wt%

x = TMPS variable length crystallizable component

z = overall molecular $\sim 10^5$

In solution grown crystals of these copolymers from 0% up to 75% wt% DMS, the DMS component was rejected to the surface. It interferes at all levels with screw dislocations growth, eventually eliminating this process, causing the crystals to more than double the original homopolymer thickness which is indicative of the interlayer disorder. At the same time crystals change from a multi-layer screw surface with well-developed faces to a ragged appearance (see Fig. 8A)—to which it is difficult to assign internal order; yet these crystals diffract in the electron beam. Based upon X-ray and DSC crystallinity measurements, the X_c declines from $\sim$75% for TMPS homopolymer to $<$50% in the copolymer

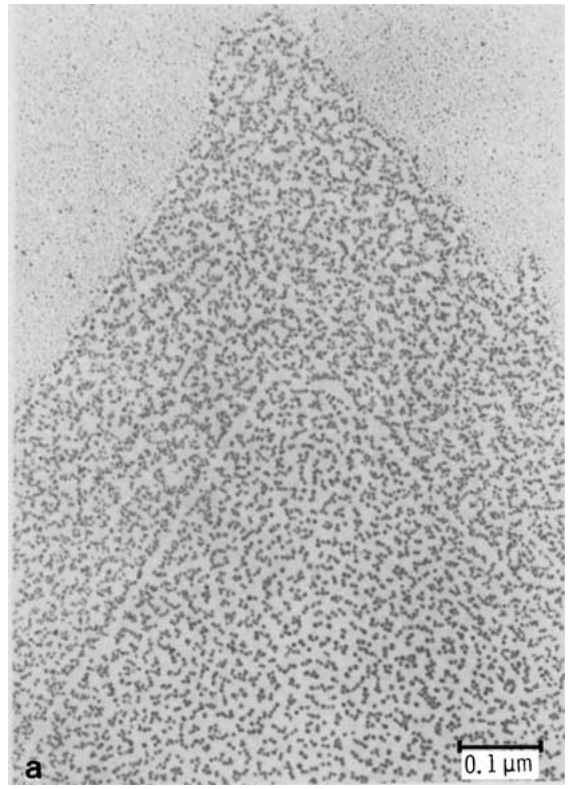

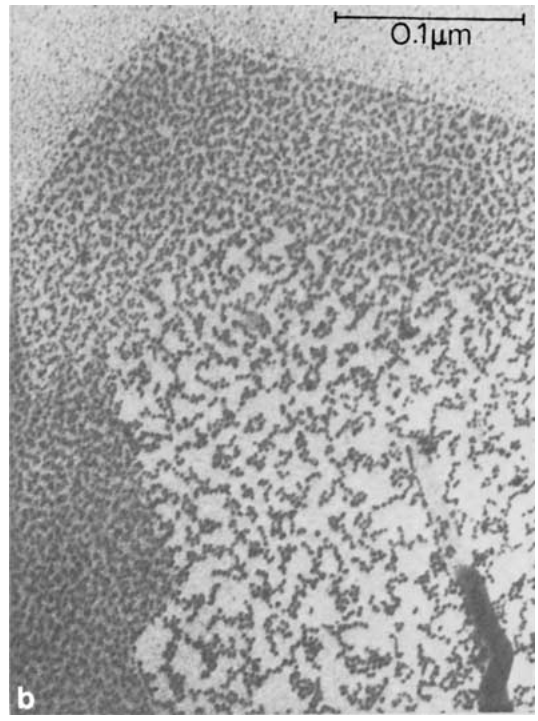

Figure 7 Gold decorated surfaces of polyethylene crystals, a) without xylene mobilization of the surface (after Bassett *et al*., 1967), and b) after mobilization of the crystal surface (after Blundell and Keller, 1973).

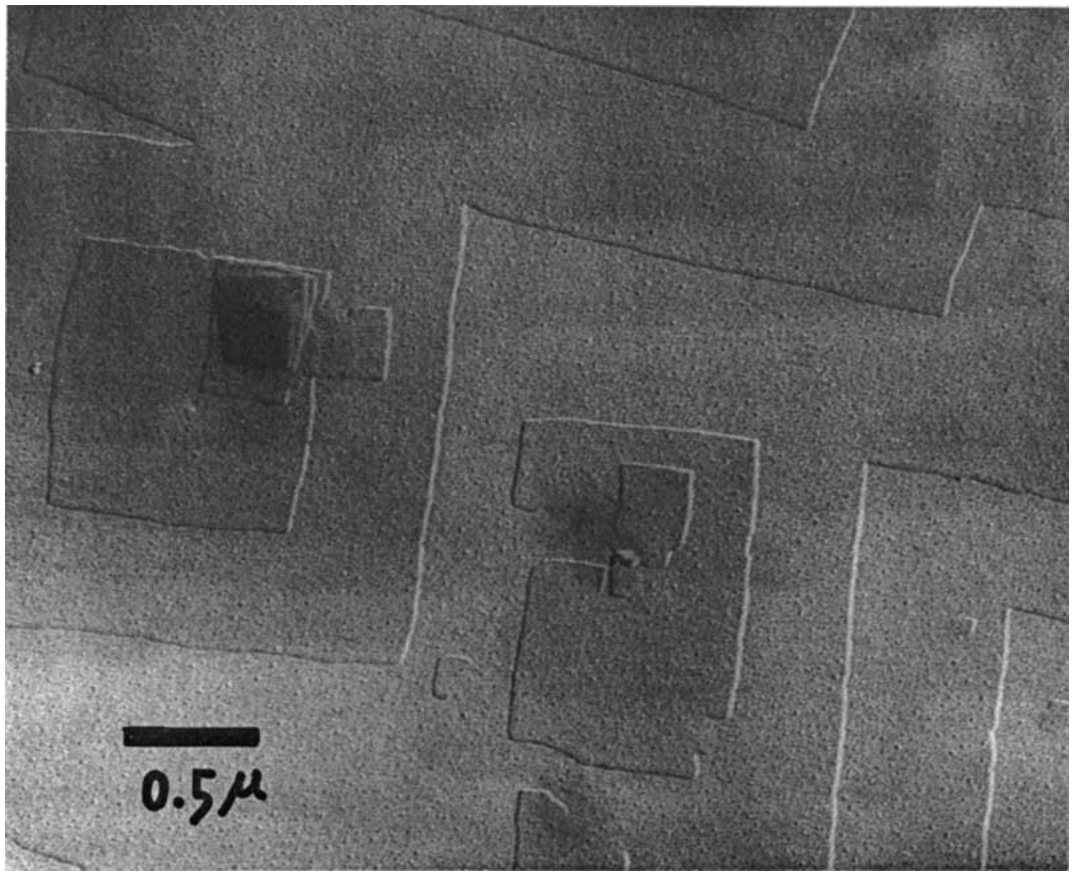

(a)

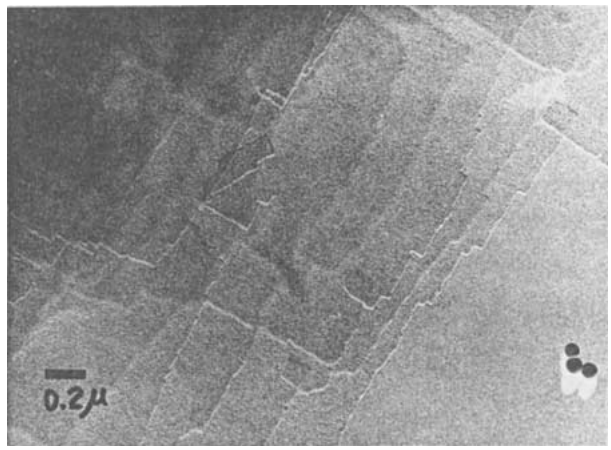

(b)

Figure 8A Solution growth poly (TMPS/DMS) crystals of different wt.% DMS block copolymers listed in Fig. 8B; after Refs 81). (*Continued*.)

with the highest DMS content. An even greater decrease occurs when the same copolymers are melt crystallized. The spherulitic samples with crystallinity of about 13% occur for the highest DMS content of 25/75 wt% copolymer. Surprisingly the spherulite shape is much better preserved than that of the corresponding crystals. It is important to realize that an increase in interfacial free energy accompanies this decrease in X_c. Under the polarizing microscope these spherulites do not appear to exhibit this serious change in X_c (see for instance Fig. 8B). However, property measurements such as density, melting and glass temperatures, Young's modulus and dynamic storage moduli decrease. An increase in the SAXS long period and elongation with DMS content under applied stress, are all significant and inter-related [81]. The interlamellar disorder in spherulites is aggravated by topological constraints and by the rejection of non-crystalline DMS and other matter to the lamellar interfaces which accords with all of the measured trends in properties [82]. There is hardly a hint of this drastic decrease in crystallinity from an inspection of the spherulitic micrographs. Clearly, branching and all kinds of defects are rampant in most spherulites for space-filling and other reasons. The samples of lower crystallinity are somewhat elastic, yet they are linear copolymers. We already know that significant decreases in crystallinity with increasing molecular weight take place in homopolymers on account of increasing interlamellar disorder with increasing MW.

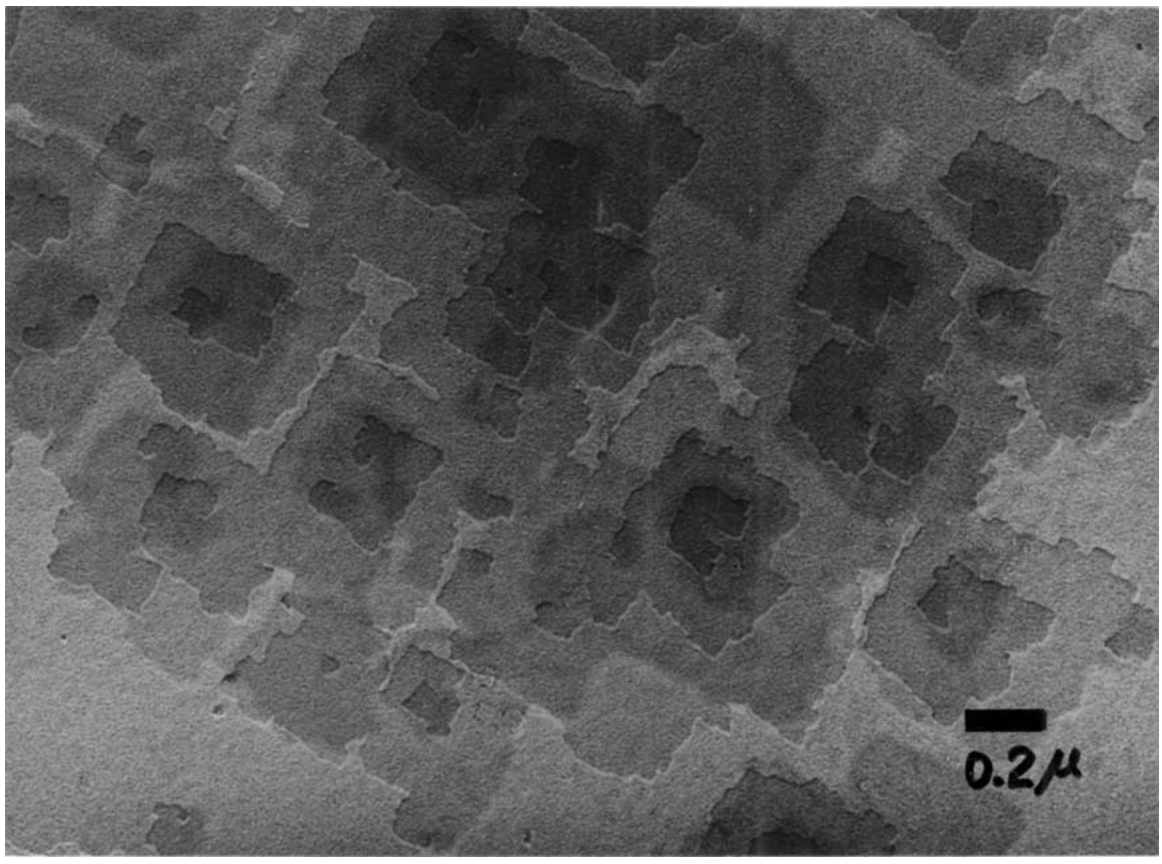

(c)

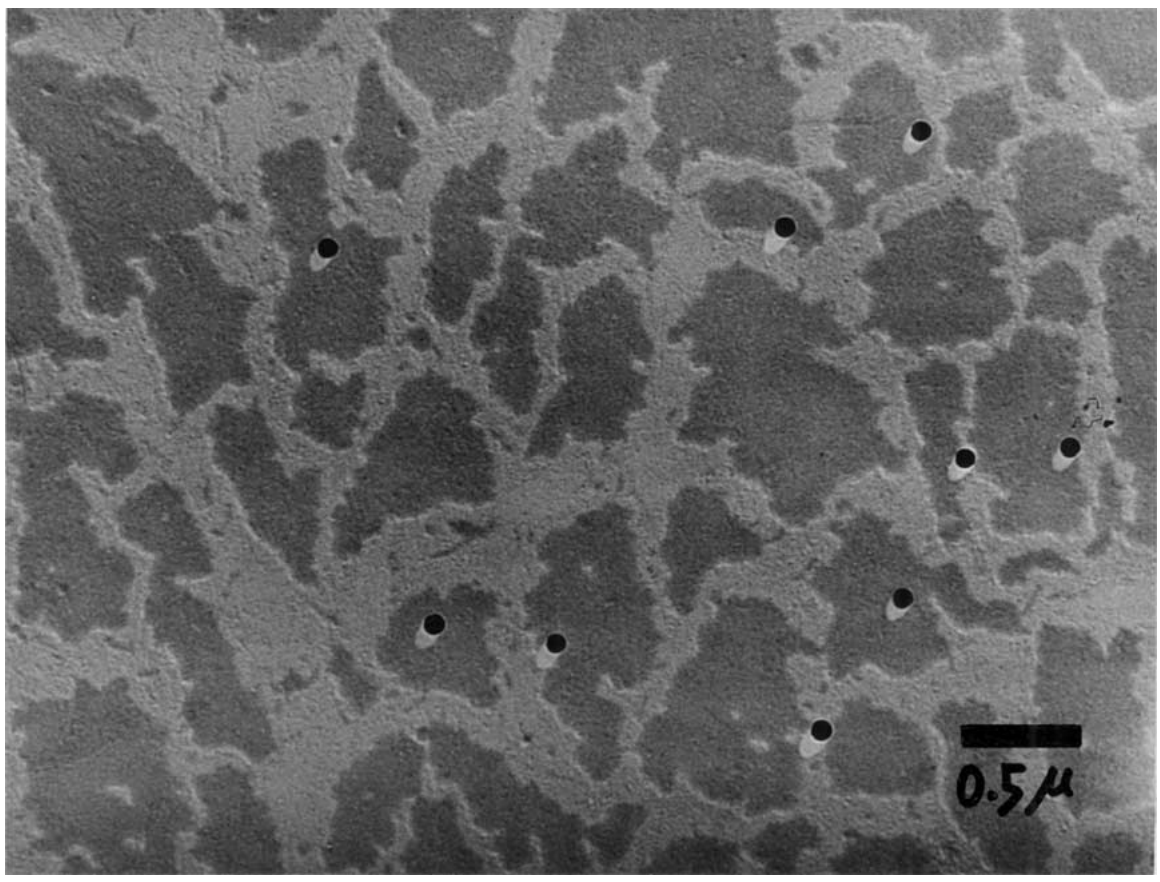

(d)

Figure 8 A (*Continued.*)

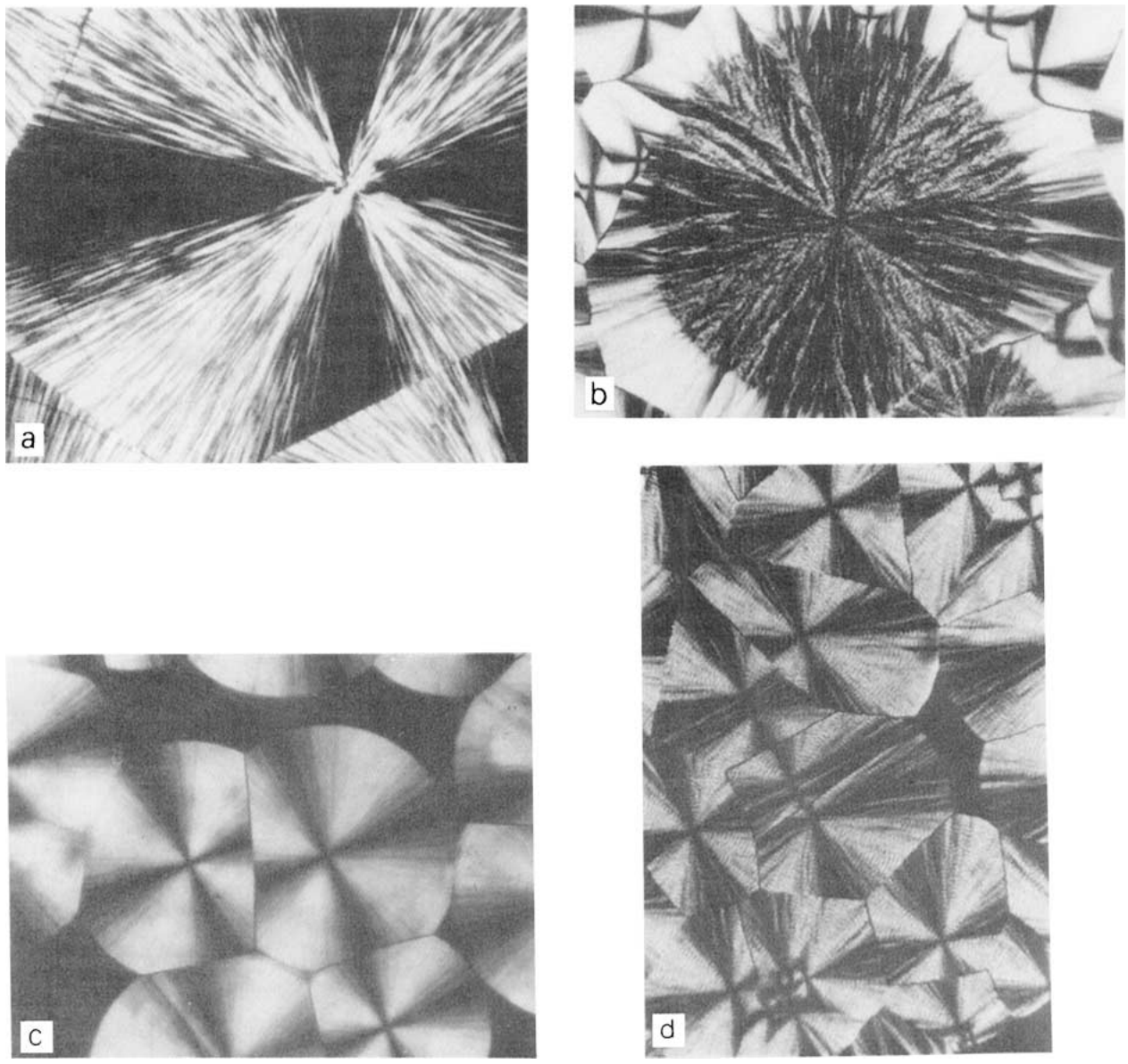

Figure 8 B Melt crystallized spherulites in random block copolymer TMPS/DMS, a) poly(TMPS) crystallized at 90°C (×380) b) TMPS/DMS (30/70 wt%) stepwise crystallized at 62.5°C and 25°C, respectively (×375) c) TMPS/DMS (50/50 wt%) crystallized at 30°C (×400) d) TMPS/DMS (50/50 wt%) crystallized at 60°C (×400); after Li and Magill, *Polymer*, **19** (1978) 815.

9. Micro-beam scattering from spherulites

Herbst [18] and Keller [19] pioneered the use of X-ray microbeams to study orientation within several kinds of spherulites such as polyethylene, polyesters, polyamides and other investigations have used this technique for the same purpose. An interesting comparison may be made of the different types of electro-magnetic scattering obtained from negatively birefringent poly (TMPS) spherulites in Fig. 9, illustrated by:

(a) 30 μm dia. X-RAY beam of Cu K_α X-ray radiation (exposure time in hours) [56].

(b) 4 μm synchrotron beam of $\lambda = 0.095$ nm (exposure time 16 s/frame) [83].

(c) 50 μm laser light beam in V_v, H_v, V_H, and H_h modes (exposure less than one minute; each pattern in this micrograph received the same exposure). At the extreme right is shown the fibrillar portion (e) of the spherulite from which the small angle light scattering SALS was obtained [84].

Diffraction patterns (a) and (b) were obtained from spherulites in an 8700 Dalton fraction and SALS depicted in (c) was obtained from a 25000 fraction spherulite. In all instances, the spherulites were large compared to the respective radiation beam diameters employed. All patterns were recorded along a spherulite radius and each depicts the morphological features corresponding to uncoordinated twisting of "rod-like" lamellae from within these spherulites. In (a) the wide angle X-ray scattering (radius arrowed) clearly shows the tetragonal symmetry that is associated with the crystal structure of poly (TMPS) [69]. The lamellae are radial with a small degree of divergence with respect to each other. In (b) the short wave-length small-angle X-ray scattering traverses the center of the spherulite from one side to another, in 5-μm step increments as marked in the figure. At the center of the spherulite where lamellae are more divergent, Riekel *et al*. [83] reported a six-point pattern where more lamellae are twisting (less ordered) with respect to each other; further out the

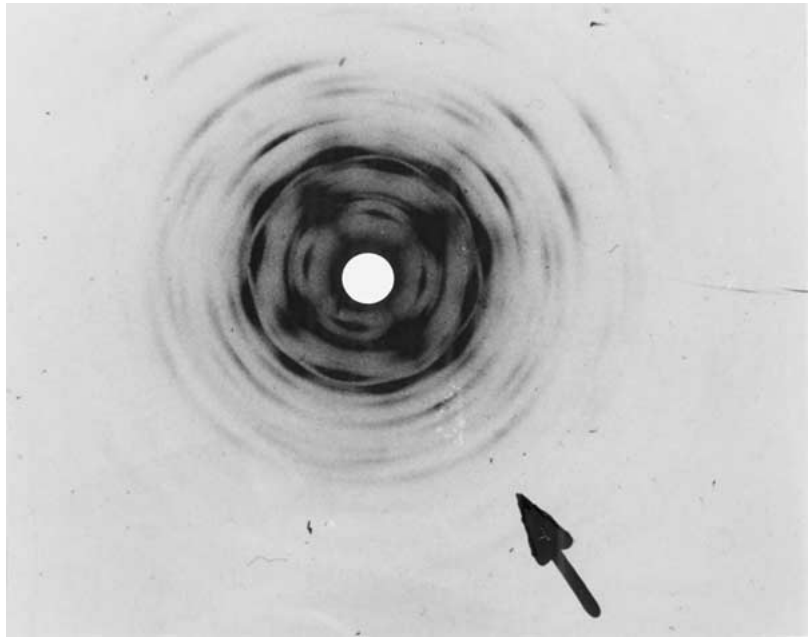

(a)

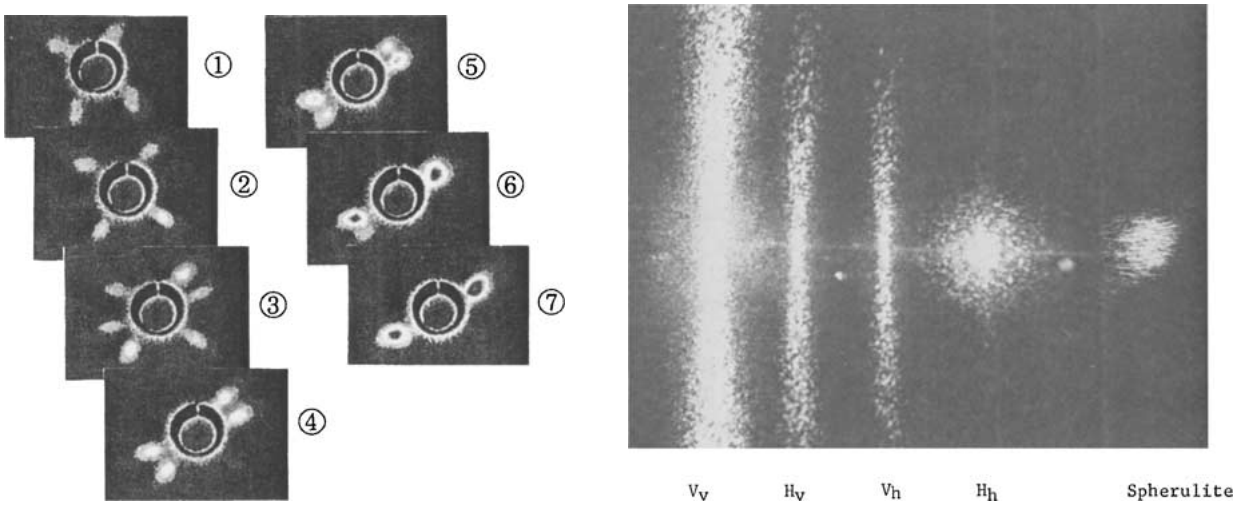

(b) (c)

Figure 9 Electromagnetic scattering from poly (TMPS) spherulites obtained from isothermally crystallized fraction of 8.7 K Daltons for i) 30 μm diameter beam of Cu K_α X-ray radiation (several hrs.); after Magill, 1964; ii) 4 μm synchotron beam of $\gamma = 0.095$ nm (exposure time 16 s/frame) Courtesy of C. Riekel); iii) 50 μm laser light beam in V_V, H_v, V_H and H_H modes (exposure less than one minute; each pattern in this micrograph received the same exposure). At the extreme right is the fibrillar portion, d) of the spherulite from which the SALS scattering was obtained; after Birnboim *et al*., Ref. 84).

scattering moves from a four-point SAXS pattern to a two-point image further out along the radius where lamellae are nearly parallel to each other. In (c) the SALS pattern taken with a 30 μm diameter beam from an area (d) of the spherulite illuminated on the extreme right. All of the scattering features were obtained along the spherulite radius, and they are consistent with a stronger polarizability perpendicular to the radius in the V_v pattern which corresponds to the growth direction of the rods or lamellae. As anticipated, it is correspondingly less for H_v and V_h scattering signals respectively. All of this is in agreement with a "c" axis orientation transverse to the lamellae that are radially oriented. The H_v pattern is almost symmetrical. In this diagram H and V refer to the polarizer and analyzed directions and the subscripts denote the plane of polarization in each instance. The elongated dark flecks that are evident between cross-polaroids from within a poly (TMPS) spherulite in the radial direction (see for instance Fig. 9(c)) attest to asynchronous lamellar twisting that takes place along the radial direction.

A critique of beam (spot) size, angular resolution, synchrotron beam damage and other key factors is given in Riekel's informative article for the ESRF micro X-ray scattering facility and other instrumentation [83] and in other papers now in press. Many different beam sizes are now used routinely at ESRF with the smallest below 100 nm diameter favored for more detailed morphological probing.

10. Void formation during crystallization

Voids are an important source of "defects" when crystallizing spherulites impinge, yet they are often overlooked, despite the fact that they may be detrimental

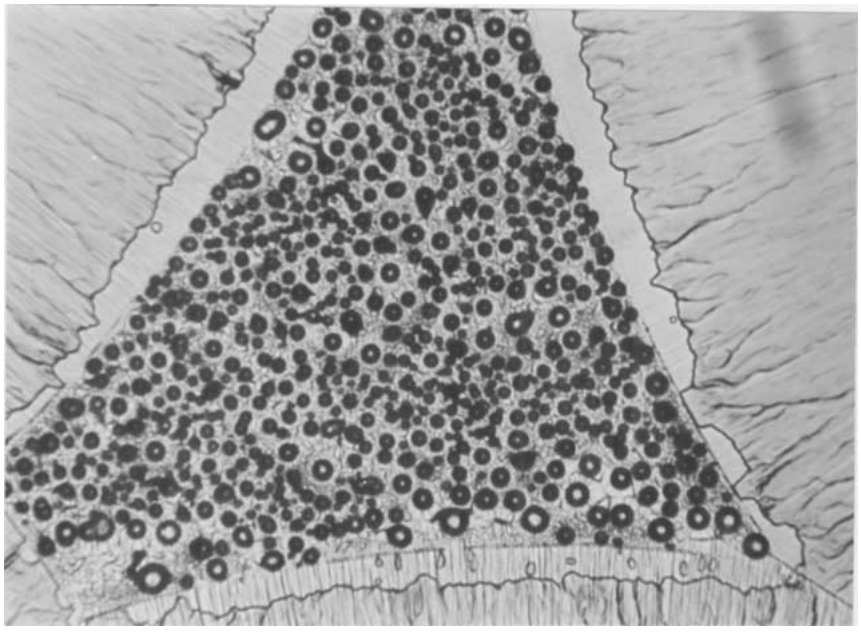

Figure 10 Void formation in entrapped melt by impinging poly (TMPS) spherulites (white light) crystallizing at 25°C (5 min) ×150; after Magill, 1964).

from a properties perspective. During crystallization numerous small voids and shorter chains may accumulate at the impinging spheruilite boundaries, especially in unfractionated polymer. A less common event, but with similar consequences arises in the isothermal crystallization of a fractionated specimen whenever relatively large spherulites entrap an isolated region of the melt as they approach each other as illustrated in Fig. 10. In order to compensate for the stressed volume in the confined space, the trapped melt undergoes prolific void formation, around which nucleation and growth occurs instantly, completely transforming the melt [56]. At the same time the peripheral regions of the larger spherulites break away from the surrounding cover slips, adding to the evidence that the enclosed volume transformation may have been stress induced. Anyhow, these encapsulated areas must impair the material density and some of its void sensitive properties. A recent and interesting example [85] of this type involves stress-induced banding in spherulites. The regular banding of the spherulites becomes distorted upon nearing an isolated melt pocket, just before void formation when nucleation is triggered. There must be many other examples of this behavior, particularly in commercial samples, that merit closer attention. Perhaps *in situ* stress measurements could be conducted during growth to investigate this situation?

11. Spherulitic thin films and crystallinity

A recent report highlights morphological changes in the crystallization of isotactic polystyrene whenever spherulitic growth is severely restricted to two dimensions i.e. in very thin layers. It is found that the resultant morphology is platelet-like or facetted in a nice illustration published by Taguchi *et al*. [86]. These authors demonstrate and ascribe the change in "habit" from facetted morphology to a dendritic-like spherulitic habit as due to diffusion-limited growth particularly at the lower crystallization conditions. All of the morphologies reported do exhibit well-defined diffraction patterns. In some sense, they are analogous to the thin polyamide films mentioned at the beginning of this article, that were reported to exhibit "single crystal-like" features by electron microscopy and diffraction, somewhat comparable with solution growth crystals. It is worth drawing attention to the fact that thick melt crystallized films of isotactic polystyrene and polyamides only exhibit moderate crystallinity levels and there is always a recognizable amorphous halo associated with discrete X-ray reflections in any such pattern.

12. Diversity in spherulite morphologies

Spherulite morphology is very dependent upon factors such as crystallization conditions, and polymer chemistry, including composition and molecular weight, as illustrated here. For instance, gutta-percha exhibits more than two types of spherulites. Fig. 4a grows isothermally with alternating bands showing two different spacings (double-extinction) with a left-hand twist from paraffin oil at 42°C., whilst Fig. 4b displays a typical Maltese cross and a fibrillar-like morphology with no banding. When trans-1,4- polyisoprene spherulites are crystallized from 1% amyl acetate solution, they appear like curved space-filling platelet-like entities emanating from a central nucleus. These spheroidal shapes (spherulites) are made up of curved multiple lamellae that may be formed by screw dislocation growth [87]. A variety of other interesting structures are to be found in Woodward's Book, Ref # 9. The morphological features of spherulite growth in rubber have been fairly well investigated but their nucleation mechanism is still unclear, as well as their growth patterns that are formed under quiescent conditions. Growth under applied tension adds a new dimension to this morphology which cannot be examined here.

In polyamides, for example, spherulitic crystallization may be categorized according to the type and sequences of the monomer repeat units in the polymer chain, as well as upon the disposition and number of H-bonds in the structure. It is customary to list the number of carbon atoms in the diamine before the number in diacid of the monomer repeat (now often written as n_1, $n_2 + 2$) for describing these polyamides. The sequencing in the unit cell and in the crystallites dictate the H-bonding and properties of a polyamide. Considerable, yet insufficient attention has been devoted to the spherulitic morphology of polyamides. Only a few "odd-odd" type polymers will be addressed here to illustrate the similarity and the diversity in this category. Nylon 5,5, nylon 5,7 and nylon 7,7, nylon 9,7 and nylon 9,9 are selected.

There is a generalized isothermal spherulite growth patterns with temperature that is portrayed in Fig 11a. In this example, the three polymers were each fused at 270°C and subsequently crystallized isothermally at different temperatures [88]. Nylon 7,7 exhibits banded spherulites below an isothermal growth temperature, T_1, where non-birefringent spherulites only crystallize. Note that the ring spacing decreases with increasing undercooling, a normal feature for most polymers. Nylon 5,5 and nylon 5,7 do not exhibit banding over the isothermal field of study, but non-banded structures occur above T_1. All spherulites are negatively birefringent on either side of T_1. The higher melting crystalline aggregates (CA) and/or hedrites nucleate and grow only at the smaller undercooling. In all polyamides studied the CA textures melt higher than either the negative

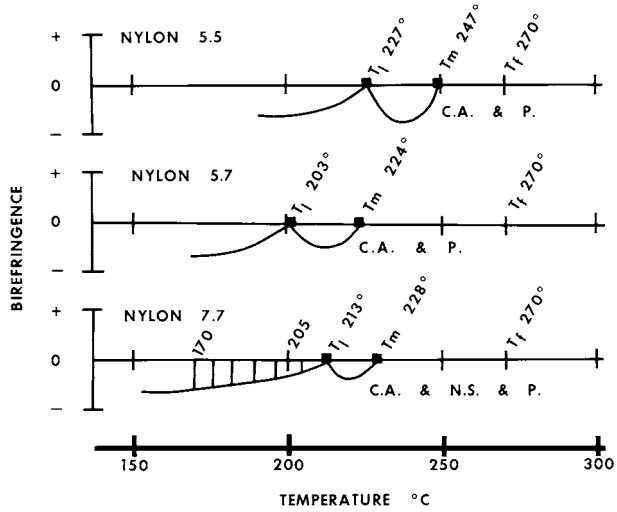

(a)

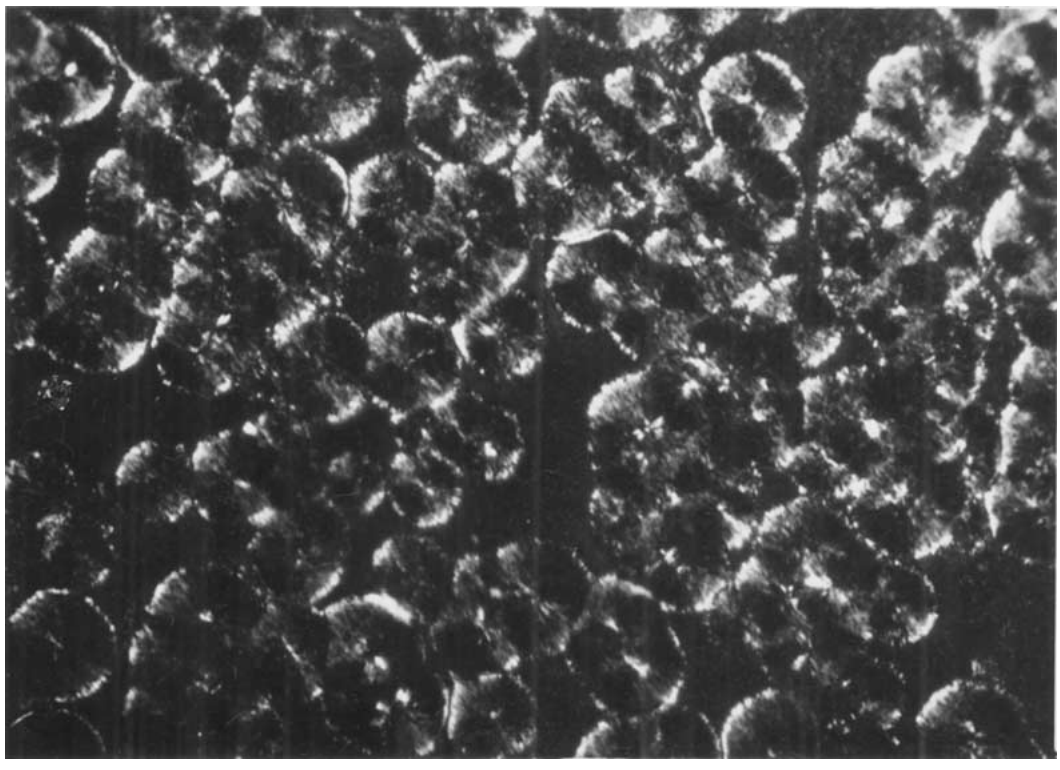

(b)

Figure 11 a) Birefringence vs. crystallization scenario for "odd-odd" polyamides: 5.5, 5.7 and 7.7. Note that all spherulites are negatively birefringent; b) displays weakly negatively birefringent spherulites grown close to T_1 in (a) (compensated mildly with a Berek compensator), ×310; c) "Mixed" spherulites of nylon 9.7 with ringed centers (3.8 μm spacing) with an aggregate-like overgrowth; crystallized at 200°C (16 hr.) after fusion at 254°C (15 min); ×400. (after Ref. 88). (*Continued*.)

(c)

Figure 11 (*Continued*.)

of positive spherulites of the same polymer. This behavior is typical of polyamides in general. All of the "odd-odd" polymers may be crystallized in very thin melt films, as platelet-like moieties or domains which exhibit well defined electron diffraction patterns. The high temperature structures of odd-odd polyamides are hexagonal, i.e. in the γ conformation (first documented by Kinoshita) which has its "c" axis perpendicular to the basal plane of the unit cell, and is foreshortened along its length by an "out-plane-twist" of the >CONH< groups in each monomeric repeat [see for example Ref. 10, p. 100–101]. Recently, Bermudez *et al*. [89] reported that solution grown crystals of 3,5 and 5,7 polyamides have H-bonds in sheets, although modeling studies determine that nylon 5,7 prefers a γ-form with H- bonding in two directions. The unusually large 50 μm spacing found in nylon 7,7 spherulites (Fig. 12) was investigated radially with a 25 μm dia Cu K_α X-ray beam. The diffraction pattern rotated in a manner consistent with lamellar twisting about an optic axis [90]. Nylon 9,7 (Fig. 11c) exhibits complex behavior with ringed centers fanning into aggregate-like overgrowths lacking well-defined extinction directions. In Fig. 11b nylon 5,5 low negatively birefringent orientation (revealed by a Berek compensator) *along* with peripheral overgrowths presumably formed upon quenching. Nylon 9,7 exhibited widely banded and "mixed" spherulites co-existing. Nylon 9,9 also showed varieties that are related to the others in this category. Elsewhere, other polyamides display a richness of detail in other categories that merit further investigation.

13. Growth morphology models

In brief, there appear to be two prominent models for ringed and non-ringed spherulites at present. Bassett's model [91] involves enhancement of rotation at dislocations through splaying of isolated lamellae. During crystallization it is stated that there is a force, exerted by (dynamic) cilia controlling morphology. In this model spherulites and chain-folding are interrelated which is inconsistent with the writer's own observations for supercooled melts of several purified aromatic molecules. Here spherulites may also grow where chains do not exist; see Section 15 of this article. The writer suggests that the viscosity of the melt may have a more tangible influence on morphology since the melt viscosity of short chain polyethylenes where C_{294} alkane spherulites are reported is of the order of a few hundred poise. This viscosity was estimated from data in the literature [92]. Surprisingly, it is about this level where spherulites were reported to grow in polyphenyl melts many years ago by the writer and associates [6]. This may be more than a coincidence. We will return to this point later, in the section on small molecule spherulites. Bassett also claims that cellulation (ie. fingering at the interface) has been recently demonstrated for the first time in his laboratory for undoped, but branched *Ziegler-Natta* type (*metallocene*) polyethylenes. Interestingly, after a period of normal linear growth, the rate becomes non-linear (decreases) as rejected species accumulate at/in the growth front, especially when the polymer branch point density is high; ie., typically ~30/1000 C atoms. A change of supercooling with

Figure 12 Melt crystallized nylon 7.7 spherulites with 50 μm spacing crystallized isothermally from the melt at 187°C after fusion at 260°C (30 min.) (unpublished).

crystallization time at the crystallization front, seems plausible enough to account for the "fall-off" in growth rate with time. However the writer is unclear about the the influence of "the force of cilia" which he believes should decrease as the MW of the polymer increases, so that its influence (this force) ought to weaken as chains increase in length. Flory *et al*. [93] demonstrated long ago that polymer properties (density, melting temperature and glass temperature etc), curve or move asymptotically towards a limiting value at high MWs.

According to the Keith and Padden phenomenological model [94], impurities are claimed to "regulate" the lamellar/fibrillar width "δ" of lamellae developing at the melt-liquid interface during spherulitic growth. The mean width, "δ", was predicted to scale as the diffusion constant D of the slower moving impurities at the front of the growing spherulite, of growth rate G, but there is disagreement between measured and predicted widths of several orders of magnitude for spherulites found in polymers and small molecules [6]. Fibrils or lamellae do become coarser as the crystallization temperature is raised in line with the model:

$$\delta = D/G \tag{4}$$

which suggests the correct trend, but not the proper magnitude of σ. The real answer may be more complex. Anyhow, there seems to be some agreement on brancing behavior *per se* between these two models, but controversy continues over finer details. Perhaps, it is appropriate to mention another complication here, ie a serious bifurcation in the Stokes-Einstein equation relating viscosity with diffusivity (which begins at supercoolings well above the respective glass temperature of several polyphenyls). This discrepancy was pointed out decades ago and re-analyzed just recently by us [95]. This bifurcation may also have serious implications for the transport term in kinetic theories of crystallization. These are inquiring rather than critical remarks.

14. Deformation of spherulites

Their mode of deformation is closely allied with the spherulitic morphology in unoriented specimens. However there are also spherulitic size effects and sample preparation, not forgetting the influence of molecular weight or copolymer content. As an illustration (not a generalization) Way *et al*. [96] have demonstrated that the yield stress for isotactic polypropylene is a function of spherulite size arising from a balance between (a) boundary failure and (b) intraspherulitic failure, each of which alters in their preparation. There are other examples in the literature dating back to the early 1960s. As already emphasized, spherulite deformation changes from brittle at low MWs, to tough at moderate to high MWs. According to Peterlin [97] HMW spherulitic polyethylene cannot be stretched to high draw ratios because of its entangled nature, except in a gelled state [98]. The changes in morphology with strain from spherulites to stretched fibrillar structures have been illustrated by Samuels [99] and Peterlin [100] and the decrease of yield stress and modulus with increasing temperatures has been covered in detail by Hadley and Ward [101] and others. Even under stress-free conditions, crystallinity depends on temperature [102, 103] and is well documented for many semicrystalline polymers (Fig. 6B). Without inherent disorder of diverse kinds of polymers would exhibit poor load-bearing properties if lamellae were solely comprised of neatly folded lamellae!

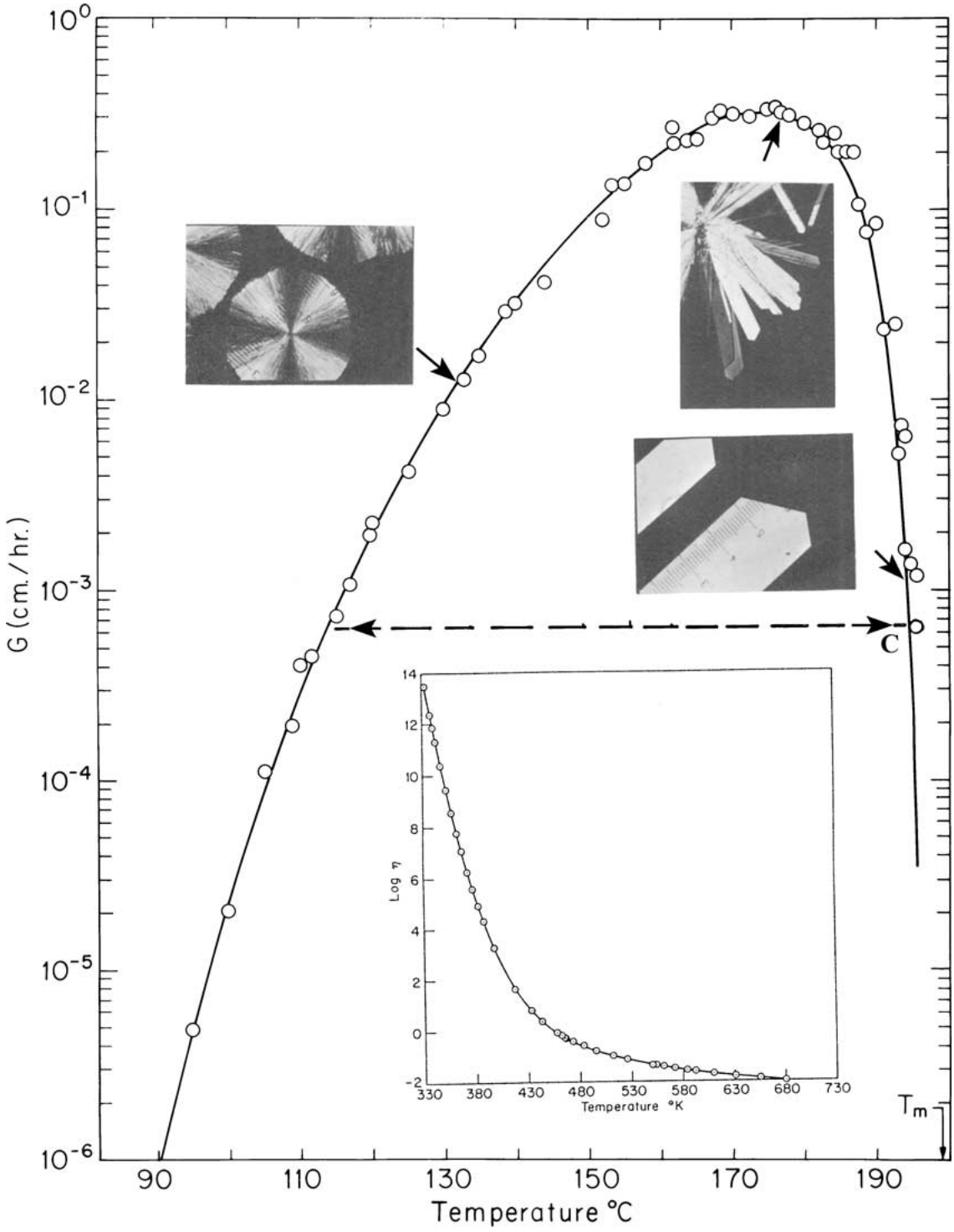

Figure 13 A Crystallization growth rate vs. temperature curve for TNB aromatic hydrocarbon with a) viscosity curve insert b) morphology inserts from simple crystals to spherulites grown from the melt. Different morphologies grow at C and D where the morphological habit can be reversed simply by changing the environment; (after Ref. 6).

15. Small molecule spherulites

Molecules form complex spatial patterns in response to a non-equilibrium situation, imposed upon them during crystallization. Systems that are in equilibrium tend to adopt simple (crystallographic) spatial structures unless they are forced out of this state by imposing a rapid change in temperature (and/or environment) when it (the system) tries to adjust itself to a lower free energy condition. This behavior may be nicely illustrated with any of the three different purified van der Waals aromatic hydrocarbons in this section. For example, consider Fig. 13A, for 1,3-bis (1-naphthyl)−5-(2-naphthyl) benzene, TNB, at small undercooling where it grows as a single crystal [6]. At large undercooling the morphology is spherulitic. For example crystallization may be rapidly down-quenched or up-quenched between any two points C and D where growth rates are identical, but the constraints very different—ie the viscosity, and/or diffusivity are magnitudes apart. If for example, a single crystal growing at C, is rapidly down-quenched to D and held here in a viscous environment, its growth front proliferates forming many smaller radial crystals

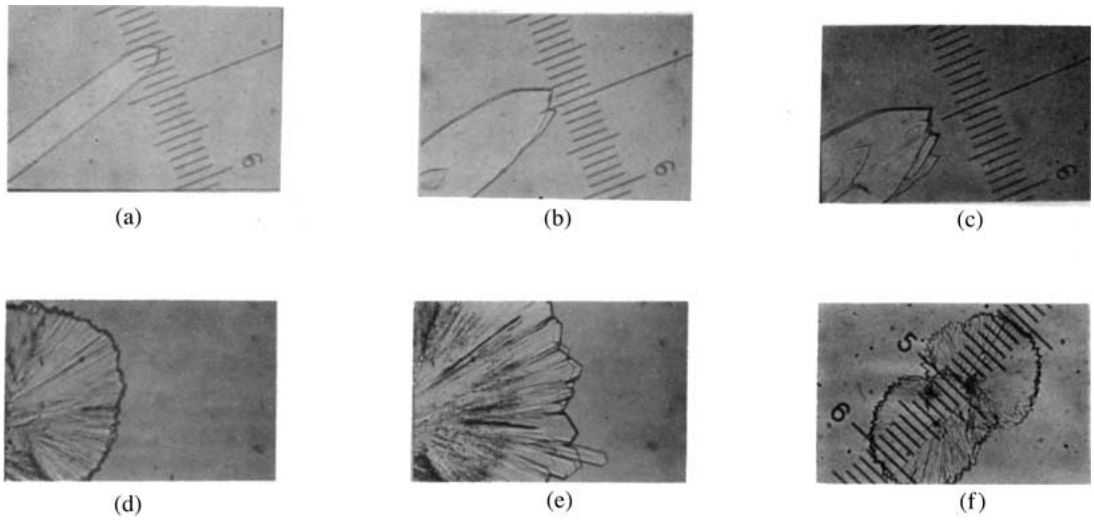

Figure 13B (a) Single crystal growth behavior of TNB (in white light) formed, for example, at C and then rapidly quenched to more viscous environment at D where (b)–(d), it develops a multi-facetted growth front fanning out into a spherulitic form. Micrograph (e) is further growth after an up-quench from (d), and (f) shows the spherulitic development at either end of the original single crystal demonstrating the overall reversibility between C and D conditions; (after Ref. 6).

that eventually take on a spherulitic morphology appropriate to its new (viscous) environment. Contrariwise, when a spherulite growing in a viscous environment at D, is switched to a low viscosity-low undercooling environment, for instance at C, and held here isothermally, it will develop well defined and facetted lamellae characteristic of the original single crystal morphology at C, but bunched together, but diverging. Fig. 13B show a time lapse series of micrographs—(a) through (f)—that illustrates this process (see figure caption). The growth pattern may be changed at will altering the growth constraints on the system. Whenever the environmental conditions are altered then the system takes on the most stable morphology appropriate to the new circumstances. This is a clear illustration of spherulite formation based entirely on environmental constraints. May be there is another reason for spherulite growth in small molecules? It seems to the writer that there are at least three factors involved, namely anisotropy, surface tension, diffusion and/or "viscous drag" governed by temperature, which are responsible for the morphology. Spherulitic formation in small molecules can only be captured in a viscous environment; and where crystallography (not impurities) is the controlling influence as just illustrated. The molecular asymmetry of the species may also play some role. Spherulites are space-filling and display a distinct Maltese cross between cross-polars. They exhibit a negative birefringence, corresponding to the lamellae (crystals) of which they are comprised. No chain-folding is necessary, only a viscous environment that relates to other important physical parameters! One of the key issues here is that the morphology depends upon the crystallization environment [6] and there only van der Waal forces between molecules are involved. Of course, small polar or ionic molecules [15] in viscous gels also yield spherulites! There are other examples of this behavior.

Dendritic morphologies also form under appropriate conditions in these asymmetric aromatic hydrocarbons. A case in point is Fig. 14a for the asymmetric aromatic molecule $1:1'$ binaphthyl ($1:1'$ DNp). This material can also exist in two distinct enantiomorphic forms, -R(−) and S-(+) depending upon the undercooling conditions. Since the melting points of each form are well separated they can be isolated from one another in selected regions of undercooling and their individual rates of crystallization measured [104]. Indeed $1,1'$ DNp can develop optical activity in a spontaneous manner [105]. Banded structures were not found in our early experiments in spite of the chirality, but spherulites were obtained, Fig. 14b. Recent investigations of banded spherulites in chiral polymers such as poly (propylene oxide) and poly (epichlorohydrin) raise some new issues between conformational chirality and handidness for further study [106]. Dendritic structures of some materials are perhaps better understood than spherulites, but we must still ask—is there a unique mechanism that is responsible for all nucleation and growth? Is a different primary nucleation and growth mechanism required for every class of materials? Surely not! Observations and measurements provide us with facts. Modeling indicates that between diffusion and surface tension the motion of a dendrite tip with emanating side branches behind it (termed secondary, tertiary etc) arises under diffusion-limited conditions. In reality, it may even be more complicated than recent computer modeling has demonstrated.

Other pure aromatic hydrocarbons that have been investigated by the writer and associates are $1:2$ diphenylbenzene ($1,2$ DPB) in some detail along with a more polar asymmetric species $\propto$-phenol-o-cresol ($\propto$POC) [105]. All of the molecules cited here are glass-formers, and it is very beneficial experimentally, that they are also crystallizable molecules that exhibit morphologies and behavior (at least superficially) not unlike more complex polar and/or polymeric species. Because of the purity of these polyphenyls, liquid and glassy properties can be investigated without interference from nucleation and crystallization within the time frame of the experimental measurements. Interestingly,

(a)

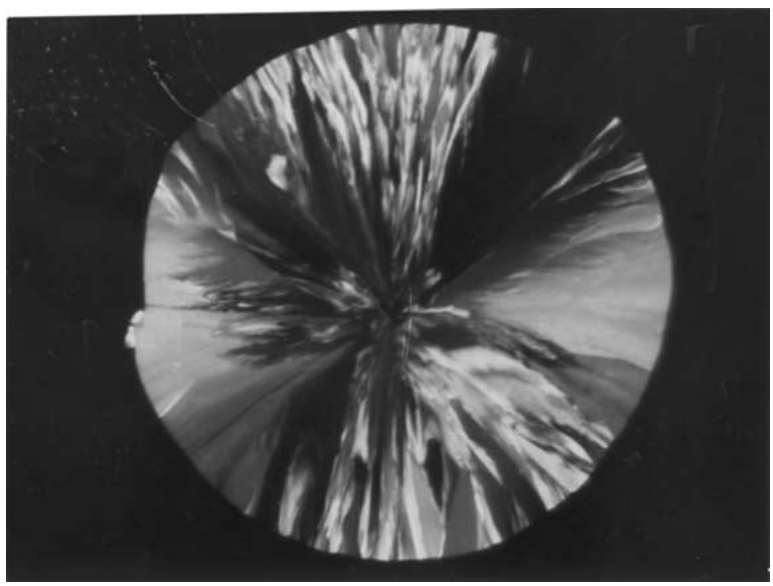

(b)

Figure 14 Crystallization of 1:1' DNp aromatic hydrocarbon crystallized from the melt a) dendrites at 120°C b) spherulite at 125°C. Scale: 1 cm = 80 μm (unpublished).

the polyphenyls all obey the rule of Jackson *et al*. [107] mentioned in our early publications which states that the interface morphology of small molecules is facetted if $\Delta S_f/R > 2$, a condition which is obeyed by the small molecules in this article. Whenever this ratio is less than 2 a planar crystal growth front cellulates (ie. breaks down into finger-like non-crystallographic proturberances). Few polymers have facetted fronts but how relevant is this ratio rule for anisotropic chains, segments or repeat units? In any case in the "link" between small and large molecules lies a challenge that still awaits an answer. Does the fact that spherulites can grow on crystals and vice-versa have any meaning?

16. Contrasts in specimen purity

For a moment it is appropriate to consider how we gauge purity in materials. Fractionation of high polymers in the melt is still problematic since zone-refining is unsuccessful on account of their high viscosity and various kinds of entanglements. It is interesting to examine some aspect of the meaning of purity in materials. Consider for example, a blend comprised of one third of each monodisperse polymer component, namely 300000, 350000 and 400000 Daltons respectively has a calculated (sharp) polydispersity index, PI. $\sim$1.01—a nice number but hardly morphologically "pure" by any standard since the highest one third of the

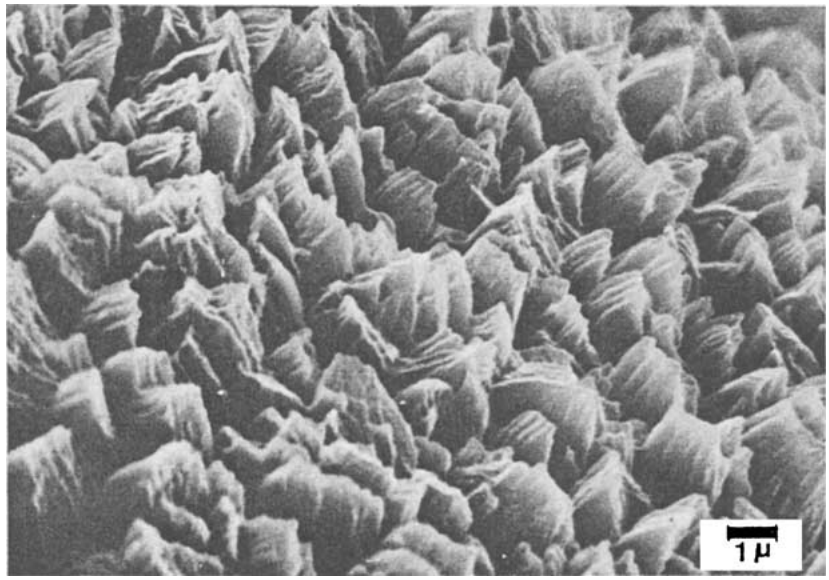

Figure 15 SEM micrograph of facetted interfaces of isotactic polypropylene highlighted by ion-bombardment after crystallized from the melt. (Courtesy of M. Kojima).

molecules are 33% longer than the lowest one third of molecules in this sample! Nevertheless some crystalline polymers have been shown to have facetted interfaces of variable shapes at the melt-substrate growth front [108] (see Fig. 15). In the case of a selenium specimen of analytical purity 99.9999% it may be comprised of Se rings and chains in equilibrium that may coexist for thermodynamic reasons [109, 110] may also exhibit facetted growth fronts! We must also wonder about the meaning and role of molecular "purity" with temperature in this and other examples.

Maybe there is a paradigm somewhere that interconnects all materials—a common thread if you will—between microscopic and macroscopic morphology if the writer was only able to recognize it?

17. Conclusions

Molecular weight is a key factor that controls spherulitic morphology and hence polymer properties and other tangible parameters. Chain length distinguishes the behavior and properties of large from small molecules, yet basic "links" in crystallization behavior seem to exist between them. The changes in properties encountered on going from low to high MWs are a consequence of topological constraints (including multiple nucleation events) at the growing substrate in the supercooled melt. In spherulites topological effects become more predominant as chains become longer. Chain folding in solution-grown lamellae is only affected at the higher molecular weights. The measured decrease in polymer density and crystallinity and the increase in interfacial free energy and toughness are in accord with other significant changes that depend upon MW in melt crystallized homo-polymers. Void formation and prolific nucleation in entrapped melt between spherulites are a potential source of weakness between spherulites. In random block copolymers of comparable MW but variable composition, non-crystallizable components segregate to inter-lamellar regions (for thermodynamic reasons) They progressively reduce and finally eliminate screw dislocations in TMPS copolymer crystals. This event is highlighted by a substantial change in morphology, increase in lamellar thickness and a decrease in crystallinity of TMPS/DMS copolymers. The biggest source of imperfections is located at crystal surfaces and spherulite inter-lamella interfaces.

In small molecules, spherulites will nucleate and grow in a viscous environment whenever circumstances are favorable. Even for relatively short monodisperse chain alkanes, spherulitic growth appears to be favored under viscous conditions. Where polymer spherulitic growth is severely limited by cover-slips, new as well as old evidence demonstrates that the morphology is more orderly here than it is when dimensional free growth is allowed. The optical appearance of spherulites cannot be used as a guide to crystallinity and other properties, yet there are groups of polymers, such as the polyamides, that seem to fit into patterns that are commensurate with their chemical structure.

References

1. G. HOLZKEY and B. MULLER, *Chem. Erde-Geochem.* **57** (1997) 277; **59** (1999) 183.
2. G. H. BROWNE and D. M. KINGSTON, *Sedimentology* **40** (1993) 467.
3. B. MIAO, D. O. NORTHWOOD, W. BIAN, K. FANG and M. H. FAN, *J. Mater. Sci.* **29** (1994) 255.
4. A. S. PELOQUIN, P. VERPAELST and J. N. LUDDEN, *Econ. Geology and Bull. Soc. Econ. Geologists* **91** (1996) 343.
5. T. MATSUNO and M. KOISHI, *J. Crystal Growth* **94** (1989) 798; M. C. COUGHLIN and B. WUNDERLICH, *J. Polym. Sci.*, part B **10** (1972) 57; *Kolloid Z. Z. Polymere* **250** (1972) 482.
6. J. H. MAGILL and D. J. PLAZEK, *J. Chem Phys.* **46** (1967) 3757.
7. P. J. BURNHAM, E. D. T. ATKINS and I. A. NIEDUSZNSKI, *Polymer* **15** (1974) 762.
8. P. H. GEIL "Polymer Single Crystals" (Wiley-Interscience: New York, 1963). Ch. 4, 223.
9. A. E. WOODWARD, "Atlas of Polymer Morphology" (OvP, 1989).
10. J. H. MAGILL, in "Treatise on Materials Science and Technology," edited by J. M. Schultz (1977) Vol. 10, pp. 181–293.
11. L. H. SPERLING, in "Encyl. Poly. Sci. Tech.," 2nd ed. (J. Wiley & Sons, New York, 1987) Vol. 9, p. 760.

12. L. L. CHAPOY, "Recent Advances in Liquid Crystalline Polymers" (Elsevier Appl. Sci. Pubs., London, New York, 1985).
13. O. LEHMANN, "Molecularphysik" (Wilhelm Guglemann, Leipzig, 1888) Vol. 1.
14. W. HECKELHAMMER, *Kunstoffe* **45** (1955) 414; A. G. M. LAST, *J. Polym. Sci.* **34** (1959) 543.
15. H. W. MORSE and J. D. H. DONNAY, *The American Mineralogist* **21** (1936) 391.
16. C. W. BUNN and T. C. ALCOCK, *Trans. Farad. Soc.* **41** (1945) 317.
17. C. W. BUNN and G. V. GARDNER, *Proc. Roy. Soc.* (London) **A189** (1947) 39.
18. M. HERBST, *Z. Elektrochem.* **54** (1950) 318.
19. A. KELLER, *J. Polym. Sci.* **17** (1955) 291, 351; **39** (1959) 151.
20. A. KELLER and J. R. S. WARING, *J. Polym. Sci.* **39** (1959) 447.
21. A. KELLER, in "Growth and Perfection of Crystals" edited by R. H. Doremus, R. N. Roberts and D. W. Turnbull (J. Wiley & Sons, Inc., New York, 1958) p. 499.
22. *Idem., J. Polym. Sci.* **39** (1959) 173; *Die Makromol. Chemie* **34** (1959) 1.
23. J. J. POINT, *Bull. Acad. R. Belg.* **41** (1955) 982, **39** (1953) 435.
24. K. HESS and H. KIESSIG, *Z. Phys, Chem.* **193** (1944) 196.
25. P. W. ANDERSON, *Science* **267** (1995) 1615.
26. A. KELLER, in "Sir Charles Frank, OBE, FRS: An Eightieth Birthday Tribute" edited by R. G. Chambers, J. E. Enderby, A. Keller, A. R. Lang and J. W. Steeds (Adam Hilger, Bristol and New York, 1991) p. 265.
27. K. H. STORKS, *J. Amer. Chem. Soc.* **60** (1938) 1753.
28. A. KELLER and A. O'CONNOR, *Nature* (1957) 1289; Discuss. Faraday Soc. **25** (1958) 114.
29. A. KELLER and D. C. BASSETT, *Proc. Roy. Microscp. Soc.* **70** (1960) 243; D. C. BASSETT and A. KELLER, *Phil Mag.* **6** (1961) 344.
30. J. I. LAURITZEN, JR. and J. D. HOFFMAN, *J. Res NBS* **64A** (1960) 73; J. D. HOFFMAN, G. T. DAVIES and J. T. LAURITZEN, JR., in "Treatise on Solid State Chemistry" edited by N. B. Hannay (Plenum Press, New York, 1976) Vol. 3, Ch. 7, p. 407.
31. R. EPPE, E. W. FISCHER and H. A. STUART, *J. Polym. Sci.* **34** (1959) 721.
32. P. H. GEIL, "Polymer Single Crystals" (Wiley-Interscience, New York, 1963) Ch. 3, p. 189.
33. J. H. MAGILL and P. H. HARRIS, *Polymer* **54** (1962), 547.
34. M. C. R. SYMONS, *J. Polym.* Part A **1** (1963) 2843.
35. C. G. CANNON and P. H. HARRIS, *J. Macromol. Sci., Phys.* **B3** (1969) 357.
36. C. RAMESH, A. KELLER and S. J. E. A. ELTINK, *Polymer* **35** (1994) 5300.
37. J. H. MAGILL, *J. Polym. Sci.*, Part A-2 **7** (1969) 123.
38. Y. FUJIWARA, *J. Appl. Polym. Sci.* **4** (1960) 10.
39. A. KELLER, *J. Polym. Sci.* **17** (1955) 291.
40. J. MANN and L. ROLDAN-GONZALEZ, *ibid.* **60** (1962) 1.
41. H. D. KEITH and F. J. PADDEN, JR., *ibid.* **39** (1959) 101, 123; **30** (1959) 1479.
42. J. F. NYE, "Physical Properties of Crystals" (Oxford University Press (Clarendon) London and New York, 1957) Ch. 13, p. 232.
43. N. A. JONES, E. D. T. ATKINS, M. H. HILL, S. J. COOPER and L. FRANCO, *Macromolecules* **30** (1997) 12, 3569; *J. Polym. Sci.* **35** (1997) 675; and others.
44. G. SCHUUR, *J. Polym. Sci.* **11** (1953) 385; F. KIRCHHOF, *Kautschuk* **5** (1929) 175.
45. M. KOJIMA and J. H. MAGILL, *Polymer* **26** (1985) 1971.
46. P. J. FLORY and A. D. MCINTYRE, *J. Polym. Sci.* **18** (1955) 592.
47. L. MANDELKERN, F. A. QUINN and P. J. FLORY, *J. Appl. Phys.* **25** (1954) 830.
48. F. P. PRICE, *J. Amer. Chem. Soc.* **74** (1955) 321; *J. Polym. Sci.* **37** (1959) 71.
49. A. SHARPLES, *Polymer* **3** (1962) 250.
50. D. M. SADLER, *ibid.* **24** (1983) 1401; *J. Chem. Phys.* **87** (1987) 1771.
51. D. M. SADLER and G. H. GILMER, *Polym. Commun.* **28** (1987) 241; *ibid.* **25** (1984) 446.
52. J. H. MAGILL, "Rates of Crystallization" in "Polymer Handbook," 4th ed. (J. Wiley and Sons, Inc., New York, 1999) Ch. VI/279.
53. L. A. WOOD and N. BEKKEDAHL, *J. Res. Nat. Bur. Stds.* **36** (1946) 489.
54. J. D. HOFFMAN and R. L. MILLER, *Polymer* **38** (1997) 3151.
55. J. H. MAGILL, *Macromol. Chem. Phys.* **199** (1998) 2378.
56. *Idem., J. Appl. Phys.* **35** (1964) 3249; *J. Polym. Sci.*, A-2 **7** (1969) 1187.
57. *Idem., Macromol. Chem.* **187** (1986) 455.
58. L. MANDELKERN, *Polym. J.* **17** (1995) 337; E. ERGOS, J. F. FATOU and L. MANDELKERN **5** (1972) 147.
59. D. R. BEECH et al., *Polymer* **13** (1972) 73 and later papers.
60. E. G. LOVERING, *J. Polym Sci.*, A2 **8** (1970) 2197; Part C **30** (1970) 329.
61. G. C. BERRY and T. G. FOX, *Ad Polym. Sci.* **5** (1968) 261.
62. J. H. MAGILL, J. M. SCHULTZ and J. S. LIN, *Colloid Polymer Sci.* **265** (1987) 193; S. S. POLLACK and J. H. MAGILL, *Polymer* **19** (1978) 411.
63. P. J. BARHAM, R. A. CHIVERS, A. KELLER, J. MARTINEZ-SALAZAAR and S. J. ORGAN, *J. Mater Sci.* **20** (1985) 1625.
64. E. A. DIMARZIO and C. M. GUTTMAN, *J. Appl. Phys.* **53** (1982) 6581.
65. Y. UDAGAWA and A. KELLER, *J. Polym. Sci.*, A-2 **9** (1971) 437.
66. K. BERGHMANN and K. NAWOTKI, *Kolloid Z. Z. Polymere* **216** (1967) 132.
67. K. BEGMANN, *ibid.* **251** (1973) 962.
68. R. KITAMARU and F. HORI, *Ad. Polym. Sci.* **26** (1978) 139.
69. K. H. GARDNER, J. H. MAGILL and E. D. T. ATKINS, *Polymer* **19** (1978) 370.
70. R. P. PALMER and A. COBBALD, *Makromol. Chem.* **74** (1964) 174.
71. A. PETERLIN and G. MEINEL, *J. Appl. Phys.* **36** (1965) 3028.
72. D. J. BLUNDELL, A. KELLER, I. M. WARD and I. J. GRANT, *J. Polym. Sci.* **B4** (1966) 781; D. J. BLUNDELL and A. KELLER, *J. Macromol. Sci. Phys.* **B7** (1973) 253; G. A. BASSETT, D. J. BLUNDELL and A. KELLER, *ibid.* **B1** (1967) 161; Y. UDAGAWA and A. KELLER, *ibid.* A-2 **9** (1971) 437.
73. T. WILLIAMS, D. J. BLUNDELL, A. KELLER and I. M. WARD, *ibid.* A-2 **6** (1968) 1613.
74. C. W. HOCK, *J. Polym. Sci.* **B3** (1965) 573; *J. Polym.* A-2 **4** (1966) 227.
75. R. ST. J. MANLEY, *J. Polym. Sci., Polym. Phys. Ed.* **12** (1974) 1347.
76. N. OKUI and J. H. MAGILL **17** (1976) 1086; N. OKUI, J. H. MAGILL and K. H. GARDNER, *J. Appl. Phys.* **48** (1977) 4116.
77. J. A. GARDELLA, JR., J. S. CHEN, J. H. MAGILL and D. M. HERCULES, *J. Amer. Chem. Soc.* **105** (1983) 4563.
78. F. KLOOS, S. GO and L. MANDELKERN, *J. Polym. Sci., Polym. Phys. Ed.* **12** (1974) 1145.
79. M. N. HALLER and J. H. MAGILL, *J. Appl. Phys.* **40** (1969) 4261.
80. M. KOJIMA and J. H. MAGILL, *J. Macromol. Sci., Phys.* **B10** (1974) 419; **B15** (1978) 63.
81. M. KOJIMA, J. H. MAGILL and R. L. MERKER, *J. Polym. Sci., Polym. Phys. Ed.* **12** (1974) 317; *J. Appl. Phys.* **45** (1974) 4159.
82. J. H. MAGILL, *J. Polymer Sci.* A-2 **7** (1969) 743.
83. A. RIEKEL, P. ENGSTROM and C. MARTIN, *J. Macromol. Sci. Phys.* **B37** (1998) 587.
84. M. H. BIRNBOIM, J. H. MAGILL and G. C. BERRY in "Electromagnetic Scattering," edited by R. L. Rowell and R. S. Stein (Gordon Breach Sci. Pubs., New York, London, Paris, p. 413. 1967).
85. H. D. KEITH and F. J. PADDEN, JR., *Macromolecules* **29** (1996) 7776.
86. K. TAGUCHI, H. MIYAJI, K. IZUMI, A. HISHINO, Y. MIYAMOTO and R. KOKAWA, *Polym. Mat. Sci Eng., Proc. Amer. Chem. Soc.*; *Sci & Eng.* **81** (1991) 308.
87. A. E. WOODWARD; courtesy of; See also Ref. 9.
88. J. H. MAGILL, *J. Polym. Sci.* A-2 **9** (1971) 815.

89. M. BERMUDIZ, S. LEON, C. ALEMAN, J. J. BORI and S. MUNOZ-GUERRA, *Macromol. Chem. Phys.* **200** (1999) 2065.
90. S. S. POLLACK and J. H. MAGILL, unpublished.
91. J. J. JANIMAK and D. C. BASSETT, *Polymer* **40** (1999) 459; C. D. BASSETT, *Macromol. Symp.* **143** (1999) 11; M. I. ABO EL MAATY, I. L. HOSIER and D. C. BASSETT, *Macromolecules* **31** (1998) 153; D. C. BASSETT, R. H. OLLEY, S. J. SUTTON and A. S. VAUGHAN, *Polymer* **37** (1996) 4993.
92. R. S. PORTER and J. F. JOHNSON, *J. Appl. Polym. Sci.* **3** (1960) 195; C. S. PEARSONS, G. DER STRATE, E. VON MEERWALL and F. S. SCHILLING, *Macromolecules* **20** (1987) 1133.
93. T. G. FOX and P. J. FLORY, *J. Appl. Phys.* **21** (1986) 2651; R. D. EVANS, H. R. MIGHTON and P. J. FLORY, *J. Amer. Chem. Soc.* **72** (1950) 2018.
94. H. D. KEITH and F. J. PADDEN, JR., *ibid.* **34** (1963) 2409.
95. K. NGAI, J. H. MAGILL and D. J. PLAZEK, *J. Chem. Phys.* **112** (2000) 1887.
96. J. L. WAY, J. R. ATKINSON and J. NUTTING, *J. Polym. Sci., Polym. Phys. Ed.* **12** (1974) 635; L. W. KLEINER, M. R. RADLOFF, J. M. SCHULTZ and T. W. CHOU, *ibid.* **12** (1974) 819.
97. A. PETERLIN, *Encycl. Polym. Sci. Tech.* **10** (1987) 26.
98. P. SMITH and P. J. LEMSTRA, *J. Polym. Sci. Polym. Phys. Ed.* **19** (1981) 1007.
99. R. J. SAMUELS, "Structured Polymer Properties" (Wiley, New York, 1974) pp. 127, 162.
100. Ref. 97, p. 80–82.
101. D. W. HADLEY and I. M. WARD, *Encycl. Poly. Sci. Technol.* **9** (1987) 379.
102. A. TURNER-JONES, J. M. AIZELWOOD, D. R. BECKETT, *Makromol. Chem.* **75** (1964) 134.
103. See R. L. MILLER, *Encyl. Poly. Sci. Technol.* **4** (1966) 449.
104. J. H. MAGILL and H. M. LI, *J. Crystal Growth* **20** (1973) 135.
105. R. E. PINCOCK and K. R. WILSON, *J. Amer. Chem. Soc.* **93** (1971) 1291; *J. Chem. Ed.* **50** (1973) 455.
106. I. SARACOVAN, H. D. KEITH, R. ST. J MANLEY and G. R. BROWN, *Macromolecules* **32** (1999) 8918.
107. K. A. JACKSON, "Liquid Metals Solidification" (J. Wiley and Sons Inc., New York, 1964).
108. M. KOJIMA, *J. Polym. Sci., Polym. Letters* **17** (1979) 609.
109. A. EISENBERG and A. V. TOBOLSKY, *J. Polym. Sci.* **46** (1960) 19.
110. B. WUNDERLICH, "Macromol. Physics" (Academic Press Inc., New York 1976) Vol. 2 Ch. 6, p. 304.

Received 25 April
and accepted 2 October 2000